C_2 SWAN BANDS IN COMETS*

RALPH E. STOCKHAUSEN AND DONALD E. OSTERBROCK†

The relative populations of the vibrational levels of the X $^3\Pi$ and A $^3\Pi$ electronic levels are calculated assuming the fluorescence mechanism. Pure vibrational transitions are taken into account by making a rough estimate of the magnetic-dipole transition probabilities. Both the approximate method, Rosseland's theory of cycles applied to a three-level molecule, and the accurate solution of the equations of statistical equilibrium for a 10-level molecule, give similar results. The excitation temperatures derived from these relative populations agree satisfactorily with the observations of the Swan bands by McKellar and Climenhaga (1953) for various sun-comet distances. Finally, an estimate is made of the infrared radiation, due to pure vibrational transitions, expected from a bright comet. The expected amount of radiation is small and will be difficult to detect.

It is well known that the C_2 Swan bands observed in comets are excited by the mechanism of resonance fluorescence (Stawikowski and Swings 1960). Observations give excitation temperatures (defined by a Boltzmann distribution of the relative populations of vibrational levels of the X $^3\Pi$ ground electronic term) in the range $T_{ex} \approx 2000$–$3000°$ at sun-comet distances of 0.48 to 1.40 a.u. (McKellar and Climenhaga 1953). Other cometary molecules such as CN, CH, NH and OH are observed to have much lower excitation temperatures, and this is understood qualitatively to be a consequence of spontaneous downward radiative transitions (vibrational and pure rotational) within the ground electronic terms of these molecules (Wurm 1936). In fact, quantitative calculations using estimated transition probabilities approximately match the observed excitation temperature (Hunaerts 1953, 1957). However C_2 has no permanent electric dipole moment, and the downward radiative transitions within the ground term are therefore forbidden, so that large populations occur in highly excited vibrational levels (Wurm 1936).

Houziaux (1960) has calculated the expected populations of successive vibrational levels in C_2, taking account only of resonance fluorescence in the Swan bands, and assuming all transition probabilities within the ground X $^3\Pi$ term to be identically zero. However the calculations do not agree very well with observation in that the calculated excitation temperatures are higher than the observed excitation temperatures and furthermore vary considerably from one level to the next.

In fact, however, magnetic dipole transitions of the type $\Delta\Sigma = \pm 1$ can occur within the ground X $^3\Pi$ term of C_2, since all the selection rules for this type of transition are fulfilled (Van Vleck 1934). We can see the approximate effect of these transitions by applying Rosseland's theory of cycles to a simplified 3 level molecule, taking the lowest levels 1 and 2 as successive vibrational levels of X $^3\Pi$, and the high level 3 as any vibrational level of the upper A $^3\Pi$ term that is connected by strong radiative transitions with both levels 1 and 2. Then the population ratio is (Ambartsumyan 1958).

$$\frac{n_2}{n_1} = We^{-h\nu 21/kT} \frac{A_{31}e^{-h\nu_{32}/kT} + \frac{A_{21}}{A_{32}}(A_{31}+A_{32})}{WA_{31}e^{-h\nu_{32}/kT} + \frac{A_{21}}{A_{32}}(A_{31}+A_{32})} \equiv e^{-h\nu 21/kT_{ex}} \quad (1)$$

where W is the dilution factor, T is the radiation temperature and T_{ex} is the observed temperature as defined above.

*Published as *Goddard Space Flight Center document X-614-64-252*, August 1964.

†Washburn Observatory, Madison, Wisconsin.

In a crude first approximation $A_{31} \approx A_{32} \gg A_{21}$ so if $WA_{31} \exp(-h\nu_{32}/kT) \gg A_{21}$, that is if the transition 2→1 is strongly forbidden, then $T_{ex} \approx T \approx 5730°$. Alternatively, if $A_{31} \exp(-h\nu_{32}/kT) \gg A_{21}$, that is 2→1 can occur, then $[W] \exp(-h\nu_{21}/kT) \approx \exp(-h\nu_{21}/kT_{ex})$. For a comet at 1 a.u. distance from the sun the geometrical dilution factor is $W \approx 5 \times 10^{-6}$, $(h\nu_{21}/kT) \approx 0.4$, and this limit gives $T_{ex} \approx 180°$. The magnetic dipole transition probability is (Condon and Shortley 1951)

$$A_{vib} = \frac{64\pi^4 \sigma^3}{3h} (aMb)^2, \qquad (2)$$

where $\sigma = 1618$ cm^{-1} is the wave number between successive vibrational levels, and (aMb) is the matrix element of the magnetic dipole moment, which we can crudely estimate to be 1 Bohr magneton. We thus roughly estimate $A_{21}(=A_{vib}) = 10^{-1}$ sec^{-1}, which is of the same order of magnitude as $WA_{31}\exp(-h\nu_{32}/kT)$, but smaller than $A_{31}\exp(-h\nu_{32}/kT)$, since for the strongest transitions in the Swan bands $A_{31} \approx 5 \times 10^6$sec^{-1}. Accordingly, we expect the calculated excitation temperature to be between the two limits above but closer to the first, that is, to be of the order of a few thousand degrees.

Therefore accurate calculations of the statistical equilibrium of cometary C_2 were made, taking into account the lowest 5 vibrational levels of the ground X $^3\Pi$ term and also the lowest 5 vibrational levels of the upper A $^3\Pi$ term.

The relative populations were obtained by solving the equations of statistical equilibrium. Equations similar to those of Houziaux (1960) were used, with the addition of pure vibrational transitions within the electronic terms. Only those pure vibrational transitions with $\Delta v = \pm 1$ were considered. For compieteness, pure vibrational absorptions of solar infrared radiation were included, although they had negligible influence on the results. Following are the equations of statistical equilibrium, lower electronic term, i = 1, 5:

$$n_{i-1} B_{i-1\ i} \rho_{i-1\ i} - n_i(B_{i\ i-1} \rho_{i\ i-1} + A_{i\ i-1} + B_{i\ i+1} \rho_{i\ i+1} + \sum_{k=6}^{10} B_{ik} \rho_{ik}) + n_{i+1} (B_{i\ i+1} \rho_{i\ i+1} + A_{i+1\ i}) + \sum_{k=6}^{10} n_k (B_{ki} \rho_{ki} + A_{ki}) = 0 \qquad (3)$$

upper electronic term, j = 6, 10:

$$n_{j-1} B_{j-1\ j} \rho_{j-1\ j} - n_j[B_{j\ j-1} \rho_{j\ j-1} + A_{j\ j-1} + B_{j\ j+1} \rho_{j\ j+1} + \sum_{=1}^{5} (B_j \rho_j + A_j)] + n_{j+1} (B_{j+1\ j} \rho_{j+1\ j} + A_{j+1\ j}) + \sum_{=1}^{5} n B_j \rho_j = 0 \qquad (4)$$

The notation is essentially the same as used by Houziaux (1960).

The same values of A_{vib} were used for all vibrational transitions of both upper and lower electronic terms. For the pure vibrational absorptions, all upper levels were assumed to absorb at $\lambda = 5.70\mu$ while the lower absorbed at 6.18μ (these are wavelengths of the $v=0$ to $v=1$ transitions). The solar radiation at these wavelengths was obtained from Allen (1963). Values of the other parameters used in equations (3) and (4) are listed in Table 1. The columns headed m and n refer to the subscripts used in equations (3) and (4). The transition probabilities were computed from the overlap integrals and the oscillator strength using the same values of these quantities as Houziaux (1960). The radiation densities were derived from the "mean monochromatic intensities" in Table 1 of Minnaert (1953). The transition probabilities and radiation densities computed here are slightly different from those of Houziaux, but either set of values gives essentially the same results.

The equations of statistical equilibrium were solved with the aid of an electronic computer. For comparison, we show in Table 2 the results of our work for the case with $A_{vib} = 0$ and a sun-comet distance of 0.72 a.u. (which is probably the distance used by Houziaux) and Houziaux's results for the same case. We believe that there is some error in the latter. Table 3 shows the results for various values of A_{vib} and the sun-comet distance. In order to allow for uncertainties in the value of A_{vib}, calculations were made with the assumed values $A_{vib} = 1.0$, 0.1 and 0.01 sec^{-1}.

It can be seen that the results of Table 3 have the same behavior as the three-level case, i.e., decreasing vibrational temperature with increasing vibrational transition probability. It is also seen that transition probabilities between $A_{vib} = 0.1$ and 1.0 sec^{-1} give excitation temperatures in the 2000–3000° range observed by McKellar and Climenhaga.

TABLE 1.—*Parameters Used in the Equations of Statistical Equilibrium*

v'	v''	m	n	λ	$A_{v'v''}$ $\sec^{-1}$	$B_{v'v''}$ $\text{erg}^{-1}\text{cm}^3\sec^{-2}$	$\rho_{v'v''}$(0.72 a.u.) erg cm^{-3} sec
0	0	6	1	5165	$6.36\cdot 10^{6}$	$5.26\cdot 10^{18}$	$1.135\cdot 10^{-19}$
0	1	6	2	5635	$1.41\cdot 10^{6}$	$1.52\cdot 10^{18}$	1.257
0	2	6	3	6191	$2.12\cdot 10^{5}$	$3.02\cdot 10^{17}$	1.433
1	0	7	1	4737	$2.67\cdot 10^{6}$	$1.71\cdot 10^{18}$	1.020
1	1	7	2	5129	$3.23\cdot 10^{6}$	$2.61\cdot 10^{18}$	1.129
1	2	7	3	5585	$1.93\cdot 10^{6}$	$2.02\cdot 10^{18}$	1.263
1	3	7	4	6122	$4.60\cdot 10^{5}$	$6.34\cdot 10^{17}$	1.425
1	4	7	5	6764	$7.75\cdot 10^{4}$	$1.44\cdot 10^{17}$	1.530
2	0	8	1	4382	$3.42\cdot 10^{5}$	$1.73\cdot 10^{17}$	0.741
2	1	8	2	4715	$4.07\cdot 10^{6}$	$2.56\cdot 10^{18}$	1.009
2	2	8	3	5098	$1.47\cdot 10^{6}$	$1.17\cdot 10^{18}$	1.096
2	3	8	4	5540	$1.96\cdot 10^{6}$	$2.02\cdot 10^{18}$	1.223
2	4	8	5	6060	$6.68\cdot 10^{5}$	$8.93\cdot 10^{17}$	1.418
3	1	9	2	4371	$8.61\cdot 10^{5}$	$4.32\cdot 10^{17}$	0.737
3	2	9	3	4697	$4.68\cdot 10^{6}$	$2.92\cdot 10^{18}$	1.001
3	3	9	4	5071	$5.24\cdot 10^{5}$	$4.10\cdot 10^{17}$	1.119
3	4	9	5	5502	$1.89\cdot 10^{6}$	$1.89\cdot 10^{18}$	1.211
4	2	10	3	4365	$1.40\cdot 10^{6}$	$6.98\cdot 10^{17}$	0.734
4	3	10	4	4685	$4.98\cdot 10^{6}$	$3.07\cdot 10^{18}$	0.995

TABLE 2.—*Relative Populations*

THIS PAPER				HOUZIAUX (1960)			
Lower Electronic Term		Upper Electronic Term		Lower Electronic Term		Upper Electronic Term	
v''	$N(v'')/N(v''=0)$	v'	$N(v')/N(v''=0)$	v''	$N(v'')/N(v''=0)$	v'	$N(v')/N(v''=0)$
1	0.69	0	$9.4\cdot 10^{-8}$	1	0.95	0	$1.0\cdot 10^{-7}$
2	0.48	1	6.4	2	0.71	1	$8.7\cdot 10^{-8}$
3	0.33	2	4.3	3	0.61	2	7.9
4	0.23	3	2.9	4	0.37	3	4.5
		4	2.0			4	6.1

From the relative populations given in Table 3 it is also possible to estimate the expected infrared radiation of cometary C_2. We will make this calculation for the (1,0) band of the lower electronic term, which occurs at 6.18μ. Both the earth-comet and sun-comet distances are taken as 1 a.u.

According to Wurm (1963), the number of C_2 molecules in the ground state of a typical bright comet is

$$N(C) \approx 6\times 10^{32} \text{ molecules}$$

The luminosity in the (1,0) band is then given by the expression

$$L \approx \frac{N(v''=1)}{N(v''=0)} \cdot N(C_2) A_{vib}\, h\nu_{vib}$$

where $N(v''=1)/N(v''=0)$ is a relative population given in Table 3. With the assumption $A_{vib}=0.1$ $\sec^{-1}$ we obtain $L \approx 9\times 10^{18}$ ergs/sec, or a flux received at the earth, assuming the whole comet is in the field of the telescope, of about 3×10^{-9} ergs/cm^2 sec.

TABLE 3.—*Relative Populations and Boltzmann Temperatures*

Lower Level		T	Upper Level	
v''	$N(v'')/N(v''=0)$		v'	$N(v')/N(v'=0)$
		$R=0.4$ a.u. $A_{vib}=1.0$		
1	0.39	25×10^2	1	0.50
2	0.22	31	2	0.25
3	0.12	33	3	0.14
4	0.06	32	4	0.09
		$A_{vib}=0.1$		
1	0.65	53×10^2	1	0.62
2	0.44	56	2	0.42
3	0.29	56	3	0.28
4	0.20	56	4	0.19
		$A_{vib}=0.01$		
1	0.69	63×10^2	1	0.68
2	0.48	62	2	0.45
3	0.33	61	3	0.31
4	0.23	62	4	0.21
		$R=0.7$ a.u. $A_{vib}=1.0$		
1	0.20	14×10^2	1	0.39
2	0.09	19	2	0.13
3	0.04	21	3	0.06
4	0.01	21	4	0.03
		$A_{vib}=0.1$		
1	0.56	40×10^2	1	0.60
2	0.36	46	2	0.36
3	0.24	48	3	0.23
4	0.14	46	4	0.16
		$A_{vib}=0.01$		
1	0.68	60×10^2	1	0.67
2	0.47	61	2	0.45
3	0.32	60	3	0.30
4	0.22	60	4	0.20
		$R=1.0$ a.u. $A_{vib}=1.0$		
1	0.11	11×10^2	1	0.34
2	0.04	15	2	0.08
3	0.01	16	3	0.03
4	0.004	17	4	0.01
		$A_{vib}=0.1$		
1	0.47	31×10^2	1	0.55
2	0.28	37	2	0.30
3	0.17	39	3	0.18
4	0.09	38	4	0.12

TABLE 3.—*Relative Populations and Boltzmann Temperatures (Continued)*

Lower Level		T_{ex}	Upper Level	
v''	$N(v'')/N(v''=0)$		v'	$N(v')/N(v'=0)$
		$A_{vib}=0.01$		
1	0.66	57×10^2	1	0.66
2	0.45	58	2	0.43
3	0.30	58	3	0.29
4	0.21	58	4	0.20
		$R=1.4$ a.u. $A_{vib}=1.0$		
1	0.06	8×10^2	1	0.31
2	0.02	12	2	0.05
3	0.006	14	3	0.01
4	0.002	14	4	0.006
		$A_{vib}=0.1$		
1	0.35	22×10^2	1	0.48
2	0.19	28	2	0.22
3	0.11	31	3	0.12
4	0.05	30	4	0.08
		$A_{vib}=0.01$		
1	0.63	51×10^2	1	0.65
2	0.43	55	2	0.41
3	0.29	55	3	0.28
4	0.20	57	4	0.19

Rough calculations can be made as to the possibility of detecting this band. Assuming that the minimum power (i.e. Noise Equivalent Power) detectable by an infrared detector is about 10^{-11} watts; and that 0.1 of the power incident on the telescope reaches the detector, then it would require a telescope diameter of several hundred inches to observe this band (even above the atmosphere). Clearly, detection of the infrared lines of C_2 are not to be expected.

In summary, then, with the estimated pure vibrational transition probabilities and the assumption of the fluorescence mechanism, we have been able to derive relative populations of a 10-level C_2 molecule. These results are in agreement with those suggested by a simplified 3-level molecule and with published observations of comets.

It has also been possible to predict the infrared emission expected from a bright comet. This emission seems too weak to be observed. Similar calculations need to be performed on other cometary molecules to predict their infrared spectra.

REFERENCES

AMBARTSUMYAN, V. A. 1958, *Theoretical Astrophysics* (London: Pergamon Press), p 416.

CONDON, E. U. and SHORTLEY, G. H. 1951, *The Theory of Atomic Spectra* (Cambridge: Cambridge University Press).

HOUZIAUX, L. 1960, Ann d'ap., **23**, 1025.

HUNAERTS, J. 1953, Mem. Soc. R. Sci. Liege, **13**, 59.

HUNAERTS, J. 1957, Mem. Soc. R. Sci. Liege, **18**, 82.

MCKELLAR, A., and CHAMBENHAGA, J. L. 1953 *La Physique des Comètes* (Rept. of 4th Liege Symposium).

MINNAERT, M. 1953, *The Sun* (Chicago: University of Chicago Press), 92.

STAWIKOWSKI, A., and SWINGS, P. 1960, Ann d'ap., **23**, 585.

VAN VLECK, 1934, Ap. J., **80**, 161.

WURM, K. 1936, *Handbuch der Physik*, **7**, 306.

WURM, K. 1963, *The Moom, Meteorites and Comets* (Chicago: University of Chicago Press)

EVOLUTION OF O STARS. II. HYDROGEN EXHAUSTION AND GRAVITATIONAL CONTRACTION*

RICHARD STOTHERS

The evolution of a star of 30 $M_\odot$ is considered from the end of the stable phase of hydrogen burning to the onset of helium burning. Ten models are constructed for the hydrogen-exhaustion (E) phase, and six models for the gravitational contraction (G) phase.

The time scale of the E-phase is so short (8.8×10^4 years) that the shell source remains peaked at $q=0.34$ and undergoes little hydrogen depletion. Because radiation pressure remains strong in the core, convection does not vanish when the hydrogen content at the center falls to zero. Gravitational contraction of the core contributes more to the luminosity than shell burning, but since the total luminosity changes little, the structure of the envelope is hardly affected. On the H–R diagram, the evolutionary track turns back toward the main sequence when $X_c=0.03$, and does not turn away again until the shell source becomes important.

The G-phase begins when $L_{H,\,core}/L<0.001$, and lasts 9×10^3 years. Although the temperature in the shell increases, hydrogen depletion remains negligible because of the short time scale. However, the shell narrows considerably and its peak moves slightly inward for a while. The steep temperature gradient outside the shell causes the semiconvective zone to move inward to $q=0.48$; the hydrogen discontinuity attains a value $\Delta X=0.1$. As the luminosity and radiation pressure in the shell simultaneously increase, the envelope expands. The shell then behaves like a node, since the core continues to contract. The convective region near the center shrinks asymptotically to a value $q=0.06$, but at no time does the core approach an isothermal condition. The gravitational energy release is nearly uniform throughout the core in all phases. At the onset of helium burning, $T_c=1.5\times10^8$ °K and $\rho_c=270$ gm/cm³. Because of the brightening shell source, the stellar radius increases rapidly, bringing the evolutionary track to completion of the typical S-shaped curve on the H–R diagram.

When helium starts to burn, the spectral type is B3, and the star is expected never to return to the region of O stars during its active life.

I. INTRODUCTION

In massive stars when the central hydrogen content falls to a value of 0.03, the whole structure undergoes a drastic reorganization. Kushwaha (1957) first considered the subsequent early phase of hydrogen burning in a shell outside the convective core for a star of 10 $M_\odot$. Reiz (1963) has reconsidered and extended this work, but Hayashi and Cameron (1962) and Hayashi, Hoshi, and Sugimoto (1962) have pursued the study of a star of $15.6M_\odot$ into the entire hydrogen-exhaustion phase and then into the gravitational contraction phase preceding helium burning. These phases have also been considered for stars of intermediate mass, as follows: $3.89M_\odot$ (Hoyle 1960), $4M_\odot$ (Hayashi, Nishida, and Sugimoto 1962; Hayashi, Hoshi, and Sugimoto 1962), $5M_\odot$ (Polak 1962), and $7M_\odot$ (Hofmeister, Kippenhahn, and Weigert 1963). It is the purpose of the present paper to follow the evolution of a star of $30M_\odot$ during these phases to the onset of helium burning at the center. The previous hydrogen-burning stage has been computed in Paper I (Stothers 1963).

II. ASSUMPTION AND DEFINITIONS

a) Assumptions

The same general assumptions as in Paper I are made, except that nuclear-energy generation also occurs in a radiative shell around the core and the

*Published in *The Astrophysical Journal*, 140(2): 510–523, August 15, 1964. This paper and "Evolution of O Stars. I Hydrogen Burning" were based on the author's doctoral dissertation, Harvard University, 1963.

time rate of change of the physical variables must be taken into account during these fast evolutionary phases.

The opacity of stellar material is again assumed to be due only to electron scattering, and the equation of state is represented by the sum of the perfect gas pressure and radiation pressure.

b) Notation

In general, we apply the same notations for stellar zones as in Paper I, except here we divide the radiative intermediate zone into outer (Zone IIIa) and inner (Zone IIIb) subzones, separated by the radiative, hydrogen-burning shell (denoted by a subscript s).

To designate the successive evolutionary phases we introduce H (hydrogen burning), E (hydrogen exhaustion), and G (gravitational contraction) followed by a number indicating the particular model in the phase.

c) Chemical Composition

The outer radiative envelope retains the initial age-zero composition assumed in Paper I:

$$X_e=0.70,\ Y_e=0.27,\ Z_e=0.03,\ X_{\rm CNO}=Z_e/2. \quad (1)$$

The semiconvective zone constantly adjusts its composition to maintain convective neutrality. A discontinuity in X marks its interface with the inner radiative zone, which retains a constant gradient in X, left behind by the retreating, homogeneous convective core. The distribution of X for the last model of the hydrogen-burning phase is given by Figures 3 and 4 of Paper I. In the core of that model $X_c=0.07$.

The change of hydrogen content as an explicit function of time, τ, and mass fraction, q, is given by

$$\frac{\partial X}{\partial \tau}=-\frac{\epsilon_{\rm H}}{E_{\rm H}} \text{(radiative region)} \quad (2)$$

and

$$\frac{\partial X}{\partial \tau}=-\frac{1}{q_4 E_{\rm H}}\int_0^{q_4}\epsilon_{\rm H}dq \text{ (convective core)}, \quad (3)$$

where $\epsilon_{\rm H}$ is the energy generation due to hydrogen burning and $E_{\rm H}=6.0\times10^{18}$ erg/gm is the energy released per CNO cycle.

d) Nuclear Energy

The accurate expression for the rate of energy release due to the conversion of hydrogen into helium via the full CNO cycle has been given by Reeves (1962) in terms of the $N^{14}+H^1$ rate:

$$\epsilon_{\rm H}=7.94\times10^{27}f_{14,1}g_{14,1}\left(\frac{X_{14}}{X_{\rm CNO}}\right)X_{\rm CNO}X\rho T_6^{-2/3} \exp\left(-152.3T_6^{-1/3}\right) \text{ erg/gm sec} \quad (4)$$

where

$$f_{14,1}=1+1.75\,\rho^{1/2}T_6^{-2/3}, \quad (5)$$

$$g_{14,1}=1+0.0027\,T_6^{1/3}-0.0037\,T_6^{1/6}-0.00007T_6, \quad (6)$$

$$X_{14}/X_{\rm CNO}=0.99-0.00067\,T_6. \quad (7)$$

Here $f_{14,1}$ is the weak electron-screening factor, $g_{14,1}$ is the correction term to the zero-energy S factor, and $X_{14}/X_{\rm CNO}$ has been estimated from tables given by Reeves (1962) for temperatures in excess of 2.5×10^7 °K. We are assuming everywhere the full equilibrium abundance of oxygen, which, strictly speaking, is not attained in the cooler shell source because of the short time scale involved.

e) Gravitational Energy

The amount of energy involved during a gravitational contraction or expansion is expressed as the difference between the work done by the pressure and the change in thermal energy of the gas and radiation:

$$\epsilon_g=-P\frac{\partial v}{\partial s}-\frac{\partial u}{\partial \tau}=\frac{3kT}{2\mu H}\left[\frac{\partial}{\partial \tau}\ln\left(Ty^{-2/3}e^{-8y/3}\right)+\frac{5+8y}{3}\frac{\partial}{\partial \tau}\ln\mu\right], \quad (8)$$

where

$$v=\frac{1}{\rho},\qquad \frac{u}{v}=\frac{3}{2}\frac{k}{\mu H}\rho T-aT^4,\qquad y=\frac{1-\beta}{\beta}, \quad (9)$$

and the time derivative applies to a given mass fraction. As Hayashi and Cameron (1962) have noted, the logarithmic arguments in equation (8) are independent of position in convective regions of the star.

III. BASIC EQUATIONS

The basic equilibrium equations are given in Paper I. For Zones I–IIIa the equations were transformed and integrated, and the zones fitted to each other in the same way as before. Henceforth we shall call this region simply the *envelope*. It is specified only by the luminosity L (through the parameter C) since, down to the chosen termination point $q_f=0.500$, the composition in the radiative region has been fixed by the previous models.

In the *core* (Zones IIIb and IV) we employ q as the independent variable and logarithms of $r, L(r)$, P, and T as dependent variables. The core solutions are specified by β_c and T_c and are integrated from the center out through the shell to q_f, beyond which any energy sources are negligible. The customary series expansions near the center (Schwarzschild (1958), p. 114) have been modified to include radiation pressure and applied at $q=0\,002$. The step value was taken to be $\Delta q=0.001$.

Fitting of the envelope and core is made at q_f in U, V, and $L(r)=L$. Since L was expected to change little during the present evolutionary phases, it was sufficient to integrate a short series of envelopes at equally spaced intervals of L and then to interpolate values of U_f and V_f at finer intervals of L.

The change in $X(q)$ as a function of time has been given by equations (2) and (3). These may be approximated by difference equations, with the known run of (ϵ_H/X) as a function of q from the previous model. Letting ι refer to quantities of the previous model, we write in an obvious notation

$$\frac{\Delta \ln X}{\Delta \tau}=-\frac{1}{2E_H}\left[\left(\frac{\epsilon_H}{X}\right)^{\iota}+\left(\frac{\epsilon_H}{X}\right)\right]=-\Xi_r(q), \qquad (q\geq q_4^{\iota}) \quad (10)$$

$$\frac{\Delta \ln X}{\Delta \tau}=-\frac{1}{(q_4{}^{\iota}+q_4)E_H}\int_0^{q_4}\left[\left(\frac{\epsilon_H}{X}\right)^{\iota}+\left(\frac{\epsilon_H}{X}\right)\right]dq=-\Xi_c(q_4), \qquad (q_4\geq q>0) \quad (11)$$

$$\frac{\Delta \ln X}{\Delta \tau}=\Xi_r(q)+[\Xi_c(q_4)-\Xi_r(q_4)]\frac{q_4{}^{\iota}-q}{q_4{}^{\iota}-q_4}, \qquad (q_4{}^{\iota}\geq q\geq q_4) \quad (12)$$

for $q_4{}^{\iota}-q_4$ small. These approximations are slightly more accurate than those used by Haselgrove and Hoyle (1956) and by Hayashi and Cameron (1962). Outside the convective core, in which X_c is known (constant), an iterative procedure must be used to calculate X from equation (10) or equation (12), since (ϵ_H/X) depends implicitly on X through ρ. Using X from the previous model, we calculate a preliminary value of ρ and hence (ϵ_H/X). Insertion of (ϵ_H/X) into equations (10) or (12) yields a projected value of X. Repetition of this procedure yields a definitive value of X correct to the second order.

The method of producing an evolutionary step was varied according to the magnitude of the ratio of luminosity supplied by gravitational contraction to total luminosity, as follows.

a) $L_g/L<0.1$

The method of Hayashi and Cameron (1962) was adopted for this case only, although they seem to have used it up to $L_g/L\approx 0.6$. Here the part of the gravitational energy release inclosed in brackets in equation (8) is expressed as a quadratic function of q, with coefficients extrapolated from the previous models:

$$\epsilon_g=\frac{3}{2}\frac{kT}{\mu H}(a_0+a_1q+a_2q^2). \qquad (13)$$

The basic equations, where now $\epsilon=\epsilon_H+\epsilon_g$, are integrated from the center with input values of X_c, β_c, T_c, a_0, a_1, a_2, $q_4{}^{\iota}$, and the run of X^{ι} and $(\epsilon_H/X)^{\iota}$ as a function of q. At q_4, $\Delta\tau$ is determined by equation (11). When a self-consistent model is obtained, the quantity in brackets in equation (8) is computed exactly and improved values of a_0, a_1, and a_2 are obtained by least squares. Another model is integrated with the new values, but this second model is always sufficiently accurate for $L_g/L<0.1$.

b) $0.1<L_g/L<0.5$

In this case we specify X_c and estimate $\Delta\tau$ by extrapolation from the previous models. Hence ϵ_g can be computed exactly from equation (8) with the given $\Delta\tau$. In the course of integrations to find the correct β_c and T_c it is possible continually to improve $\Delta\tau$ by use of equation (11).

c) $L_g/L>0.5$

As L_g/L increases, L becomes more sensitive to ϵ_g and hence to $\Delta\tau$. To cope with the increasing difficulty of making $\Delta\tau$ converge, we choose a parameter that loses importance with increasing L_g/L, namely, X_c. In this case, we take the time step by specifying $\Delta\tau$ explicitly. With a value of X_c extrapolated from the previous models, it is possible to obtain a definitive value for X_c in the same way as for $\Delta\tau$ in Section III*b*. Eventually, when hydrogen burning ceases entirely in the shrinking convective core, we need only specify $\Delta\tau$.

IV. HYDROGEN-EXHAUSTION PHASE

The results of the computations for this phase are presented in Table 1. It is curious that the stellar radius starts to decrease, causing the star to turn back toward the main sequence in the H–R diagram, as soon as $X_c \approx 0.03$ for a broad range of stellar masses ($10 < M/M_\odot < 60$), even though the mass fractions contained in the convective core are very different (see Table 2). It is clear, however, why the radius will shrink when X_c becomes small. To maintain the luminosity, the central temperature must correspondingly increase; but since μ_c changes little, $R \sim T_c^{-1}$ from equation (10) of Paper I.

For a while hydrogen burning in the core is able, alone, to maintain the energy balance (Schwarzschild and Härm 1958). However, eventually an accelerated contraction of the core is necessary to supplement the deficient $L_{H,core}$ with a growing L_g. When the temperature becomes high enough, hydrogen burning in a shell outside the core also becomes important. It is interesting to note that in the above range of masses the peak of this shell source always coincides with the mass fraction of the convective core when $X_c \approx 0.07$, i.e., just *before* the radius starts to decrease. Table 2 shows that q_s, the peak of the shell source, is roughly half of q_0, the mass fraction of the core of the initial main-sequence model. Furthermore, q_0 itself increases by about 0.15 every time the stellar mass is doubled; this is a consequence of the increasing importance of radiation pressure (diminishing β), which extends the convective regions outward.

TABLE 1.—*Evolutionary Models of a Star of 30 $M_\odot$ during Hydrogen-Exhaustion (E) Phase*

	Models									
	1	2	3	4	5	6	7	8	9	10
log C	−3.272	−3.266	−3.264	−3.262	−3.260	−3.256	−3.252	−3.248	−3.244	−3.239
q_1	+0.717	+0.719	+0.720	+0.721	+0.721	+0.722	+0.723	+0.725	+0.728	+0.731
$q_2 = q_3$	+0.550	+0.547	+0.546	+0.545	+0.545	+0.543	+0.541	+0.539	+0.537	+0.534
X_2	+0.650	+0.647	+0.645	+0.644	+0.643	+0.640	+0.637	+0.634	+0.630	+0.627
X_3	+0.589	+0.584	+0.581	+0.579	+0.578	+0.573	+0.568	+0.564	+0.559	+0.554
q_s	+0.342	+0.342	+0.342	+0.342	+0.342	+0.342	+0.342	+0.342	+0.342	+0.342
β_s	+0.614	+0.608	+0.605	+0.605	+0.604	+0.604	+0.602	+0.600	+0.597	+0.595
log T_s	+7.436	+7.458	+7.487	+7.515	+7.542	+7.561	+7.571	+7.578	+7.584	+7.589
log $(r_s/R_\odot)$	+0.267	+0.240	+0.211	+0.181	+0.153	+0.130	+0.117	+0.107	+0.097	+0.089
q_4	+0.328	+0.320	+0.316	+0.311	+0.302	+0.282	+0.258	+0.236	+0.205	+0.182
log X_c	−1.523	−2.023	−2.523	−3.023	−3.523	−4.023	−4.523	−5.015	−5.882	−7.311
β_c	+0.564	+0.557	+0.554	+0.555	+0.555	+0.559	+0.563	+0.567	+0.572	+0.577
log T_c	+7.665	+7.696	+7.726	+7.756	+7.785	+7.808	+7.823	+7.833	+7.844	+7.854
log ρ_c	+0.701	+0.795	+0.886	+0.978	+1.066	+1.140	+1.193	+1.229	+1.272	+1.312
$L_{H,core}/L$	+0.999	+0.995	+0.985	+0.943	+0.853	+0.599	+0.319	+0.145	+0.028	+0.002
$L_{H,shell}/L$	.....	+0.001	+0.004	+0.014	+0.044	+0.094	+0.141	+0.175	+0.217	+0.249
L_g/L	+0.001	+0.004	+0.011	+0.043	+0.103	+0.307	+0.540	+0.680	+0.755	+0.749
log $(L/L_\odot)$	+5.439	+5.445	+5.447	+5.449	+5.451	+5.455	+5.459	+5.463	+5.468	+5.472
log $(R/R_\odot)$	+1.143	+1.136	+1.113	+1.090	+1.066	+1.057	+1.057	+1.062	+1.070	+1.079
log T_e	+4.548	+4.554	+4.565	+4.578	+4.590	+4.595	+4.596	+4.595	+4.592	+4.589
τ (10^4 years)	0.00	+5.91	+7.74	+8.33	+8.53	+8.60	+8.61	+8.67	+8.69	+8.72

It is for this reason, the very distance of the hydrogen-rich regions, that the temperature at $X \approx 0.07$ is low and shell burning is consequently delayed. (In massive stars, β is low not so much by virtue of high temperature as of low density.) In stars of lower mass the point at which $X_c \approx 0.07$ lies closer to the center, and shell burning begins to contribute significantly to the luminosity before the core contraction does. The critical mass for this to happen is about $20M_\odot$. If q_s is small enough that the core mass lies below the Schönberg-Chandrasekhar limit ($q \approx 0.1$), thus becoming isothermal or even degenerate, then L_ϱ may always be small. The approach to isothermality may be seen in a plot of log T against q for $5M_\odot$ (Polak 1962, Fig. 3), where $q_s = 0.11$. It may be inferred for $15.6M_\odot$ (Hayashi and Cameron 1962), where $q_s = 0.17$, since $L_{H,\,shell} > L_\varrho$ until $X_c < 0.001$. In stars with mass $\sim 1M_\odot$ (Schwarzschild and Selberg 1962), the shell source supplies practically all the luminosity outside a very large degenerate core. The critical stellar mass for the occurrence of degeneracy in the core prior to helium burning is $\sim 4M_\odot$ (Hayashi, Nishida, and Sugimoto 1962).

At $30M_\odot, q_s \gg 0.1$ and the core never even approaches an isothermal condition. Thus gravitational contraction proceeds unchecked to increase T_c in accordance with the virial theorem. The subsequent increase in ϵ_H reduces X_c to less than 1 percent. Thereafter the drop in X_c outruns the increase in T_c, and ϵ_H decreases, being supplanted by $\epsilon_\varrho \sim \partial T_c / \partial \tau$. However, hydrogen burning in the core still supplies over half the total luminosity even when X_c is as low as 10^{-4}.

The distribution of hydrogen in the central regions may be seen in Figure 1. It is clear that,

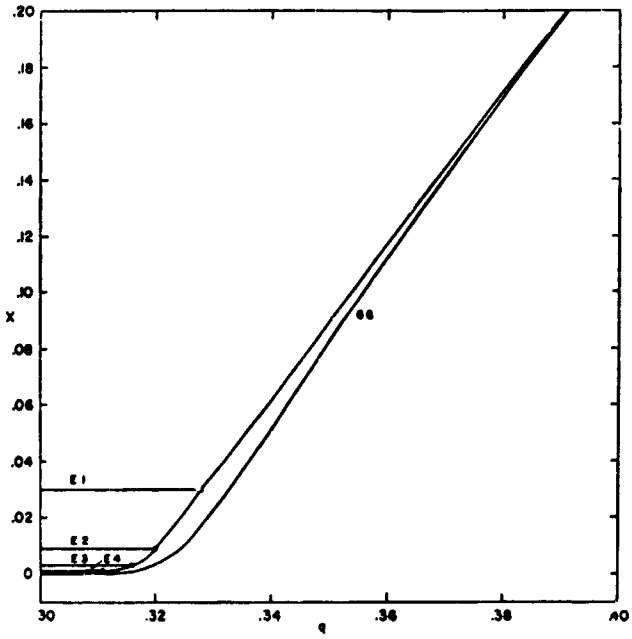

FIGURE 1.—Depletion of hydrogen as a function of mass fraction during the hydrogen-exhaustion (E) and gravitational-contraction (G) phases. Filled circles represent the boundary of the convective core in the E models.

because of the high central temperature and the luminosity requirements, X_c begins to decrease more and more rapidly with q_4. This has the effect of necessitating an even sharper increase of temperature, which consequently exhausts the central hydrogen and ignites a region which is still relatively hydrogen-rich but close enough to the center to feel the temperature rise. Thus Figure 1 shows why a shell source develops near $q = 0.34$ for $30M_\odot$. We expect this shell to be initially broader in massive stars than in stars of lower mass because the mean gradient of hydrogen throughout this region is gentler (larger $q_0 - q_s$; see

TABLE 2.—*Location of Critical Interfaces in Stars of Intermediate and High Mass When* $X_c \approx 0.03$

$M/M_\odot$	q_0	q_s	q_4	X_s	Reference
5	0.21	0.11	0.10	0.74	Polak (1962)
10	.24	.....	.07	.90	Kushwaha (1957)
15.6	.42	.17	.16	.90	Sakashita, Ōno, Hayashi (1959)
30	.60	0.34	.33	.70	Stothers (1963)
62.7	0.75	.....	0.41	0.75	Schwarzschild and Härm (1958)

Table 2). The subsequent growth of the shell source is shown in Figure 2.

In Figure 3 the relative contributions to the energy generation may be compared. The magnitude of ϵ_ϱ is very nearly constant throughout the core for all stages.

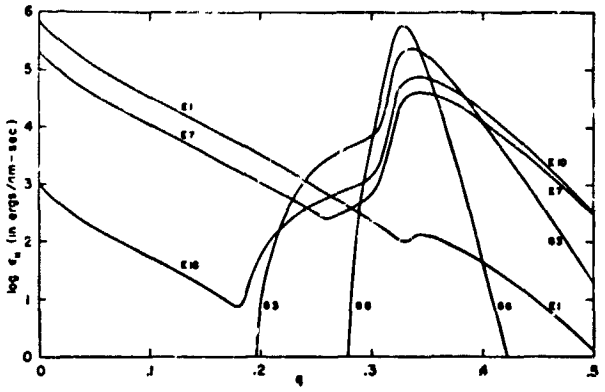

FIGURE 2.—Logarithm of the energy generation due to hydrogen burning as a function of mass fraction. Curves are labeled with the model numbers.

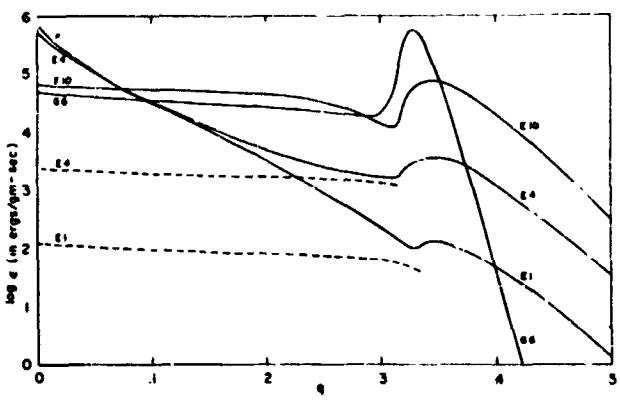

FIGURE 3.—Logarithm of the energy generation as a function of mass fraction. Solid curves refer to the contributions from both hydrogen burning and gravitational contraction. The dashed curve refers only to gravitational contraction. Curves are labeled with the model numbers.

Shrinkage of the convective core is at first slow because β_c remains almost constant. Hence the evolution of the center approximates Lane's law, $\rho_c \sim T_c^3$. When the shell source becomes important for $X_c < 10^{-4}$, ρ_c increases at a slightly greater rate than T_c^3, the only concession to isothermality that the core makes. At this point (Model E7), $L_\varrho/L \approx 0.5$ and $L_{H,\,shell}/L \approx 0.1$. It seems that as soon as L_ϱ/L grows much larger, contraction of the core begins to be offset by an expansion of the envelope (cf. Hayashi and Cameron 1962). This expansion is due to an increase of $L_{H,\,shell}$, compensating for the reduction of $L_{H,\,core}$. Exactly why the envelope expands as $L_{H,\,shell}$ increases will be made evident in the next section. The result on the H—R diagram is that the star takes another turn away from the main sequence.

When the hydrogen content at the center of the star vanishes after Model E10, the convective core does not disappear. This contrasts with the results on stars of lower mass (Hoyle 1960; Polak 1962; Hayashi and Cameron 1962), where apparently it is just the nuclear-energy generation that maintains the steep temperature gradient. However, in the case of $30M_\odot$, β is still so low that convection persists near the center.

The time scale of this phase is short enough (8.8×10^4 years) that the shell source, which remains peaked at $q_s = 0.342$, undergoes very little hydrogen depletion. Because of the struggle of the various energy sources to maintain the luminosity, L increases but slightly. Thus the structure of the envelope remains nearly constant.

V. GRAVITATIONAL CONTRACTION PHASE

This phase is taken to start when $L_{H,\,core}/L < 0.001$. The hydrogen content of the convective core is negligible, and the sole nuclear-energy source is the hydrogen-burning shell. In Model E9 the rise of the shell source had terminated the upward growth of L_ϱ/L, which reached a maximum value of 0.75. This fraction becomes all the more impressive when we compare it with 0.56 for a star of $15.6M_\odot$ (Hayashi and Cameron 1962). Table 5 shows that even at the onset of helium burning (Model G6) the contribution of gravitational contraction to the luminosity is still a sizable fraction. This suggests that for stars more massive than $30M_\odot$ hydrogen burning in a shell may not become dominant.

During the shell-burning phase, the computational difficulty of fitting models increases. The reason lies in the shift of the $U-V$ curve to the left, as seen in Figure 4. This is caused by the developing chemical inhomogeneity, which began after the initial main-sequence state, and by the shell source, which produces the leftward loop on the $U-V$ plane. Because of the short time scale, the amount of hydrogen depletion is very small

TABLE 3.—*Evolutionary Models of a Star of 30 M⊙ during Gravitational Contraction (G) Phase*

	Models					
	1	2	3	4	5	6
log C	−3.231	−3.216	−3.195	−3.178	−3.165	−3.152
q_1	+0.733	+0.739	+0.749	+0.756	+0.762	+0.769
$q_1=q_3$	+0.530	+0.522	+0.508	+0.498	+0.489	+0.481
λ_2	+0.620	+0.606	+0.582	+0.560	+0.541	+0.522
X_3	+0.542	+0.523	+0.490	+0.467	+0.445	+0.425
q_s	+0.342	+0.342	+0.338	+0.328	+0.328	+0.328
β_s	+0.589	+0.576	+0.556	+0.553	+0.553	+0.515
log T_s	+7.596	+7.607	+7.626	+7.654	+7.668	+7.683
log $(r_s/R\odot)$	+0.073	+0.048	+0.001	−0.058	−0.100	−0.142
q_4	+0.155	+0.123	+0.093	+0.078	+0.069	+0.064
β_c	+0.587	+0.604	+0.631	+0.651	+0.665	+0.674
log T_c	+7.873	+7.907	+7.971	+8.035	+8.101	+8.168
log ρ_c	+1.386	+1.520	+1.760	+1.992	+2.217	+2.433
$L_{H,\,shell}/L$	+0.307	+0.391	+0.485	+0.536	+0.561	+0.575
Lg/L	+0.693	+0.609	+0.515	+0.464	+0.439	+0.425
log $(L/L\odot)$	+5.480	+5.495	+5.516	+5.533	+5.546	+5.560
log $(R/R\odot)$	+1.098	+1.144	+1.239	+1.353	+1.492	+1.680
log T_s	+4.581	+4.562	+4.520	+4.467	+4.401	+4.310
τ (10^4 years)	0.00	+0.10	+0.30	+0.50	+0.70	+0.90

and the shell source remains peaked at roughly the same mass fraction. Since the shell provides the driving mechanism for the expanding envelope while the core is contracting, r at the outer boundary of the shell remains roughly constant. Thus it is here that the change of log r with q is greatest (see Fig. 5), that is, U is a minimum, isolating the energy-producing regions from the envelope. Unless small increments in q are taken in the numerical integrations through the shell, the solutions diverge. Since the region behaves like an outer boundary ($U_s \to 0$), V tends to blow up for small changes of the input parameters, β_c and T_c.

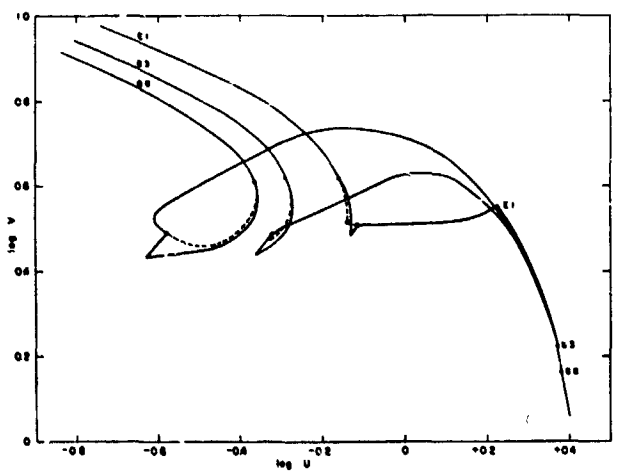

FIGURE 4.—Evolution of a star of 30 M⊙ in the U–V plane during the hydrogen-exhaustion (E) and gravitational-contraction (G) phases. Curves are labeled with the model numbers. Dots and jumps represent fitting points. The dashed lines in the solutions represent the assumed radiative zone (see Paper I).

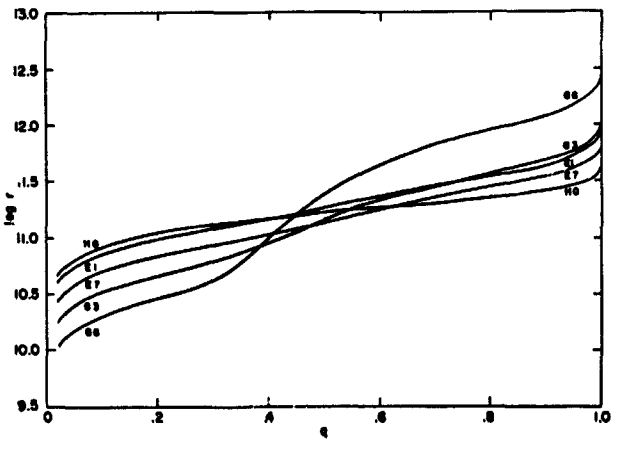

FIGURE 5.—Logarithm of the radius as a function of mass fraction. Curves are labeled with the model numbers.

Hayashi, Hoshi, and Sugimoto (1962) have interpreted the envelope expansion in terms of the $U-V$ plane. For values of the polytropic index $3 \leq N > 1$, where $P=K\rho^{1+1/N}$ and K and N are constants, the centrally condensed solutions of a polytropic envelope form a leftward loop on the $U-V$ plane and converge to a point $U=0$ and $V=N+1$ as $r \to 0$. For an electron-scattering envelope, N is 3 near the surface, decreases inside, and then approaches 3 again as $r \to 0$. Hence such an envelope approximates the polytropic case $N=3$, where $V \to 4$ as $U \to 0$ (see Fig. 4). Interior to q_s, $L(r) \ll L_{\mathrm{H,\ shell}}$ so that the radiative index becomes large, since $(n+1)_{\mathrm{rad}} \sim (1-\beta)/\kappa L(r)$. Hence the core approximates roughly the isothermal case $N=\infty$, which loops outward in the $U-V$ plane much as in Figure 4.

It remains to see how the shell source actually expands the envelope. We have already noted that, in order to tap additional nuclear fuel, the temperature in the core rises and starts shell burning. Consequent to hydrogen exhaustion in the core, the temperature in the shell must continue to rise so that $L_{\mathrm{H,\ shell}}$ can assume more of the total luminosity burden. As $L_{\mathrm{H,\ shell}}$ increases during the evolution, $(n+1)_{\mathrm{rad}}$ decreases, steepening the temperature gradient beyond q_s (see Fig. 6). But actually $n+1$ can only decrease until the adiabatic value is reached. Therefore, to compensate for the increasing luminosity, β decreases (see Fig. 7). This relative increase in radiation pressure expands the envelope.

To make this point more definite, we look at the structure of the envelope, which may be considered a polytrope of some characteristic index.

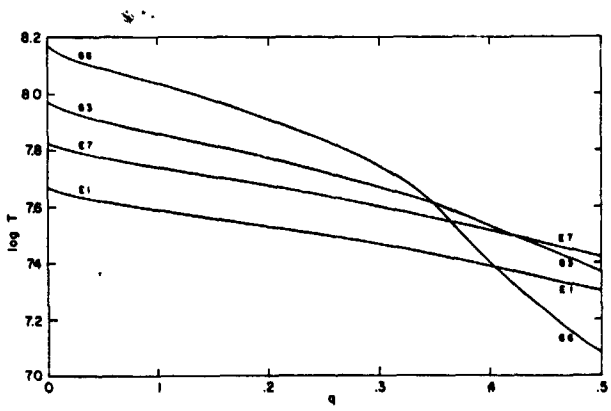

FIGURE 6.—Logarithm of the temperature as a function of mass fraction. Curves are labeled with the model numbers.

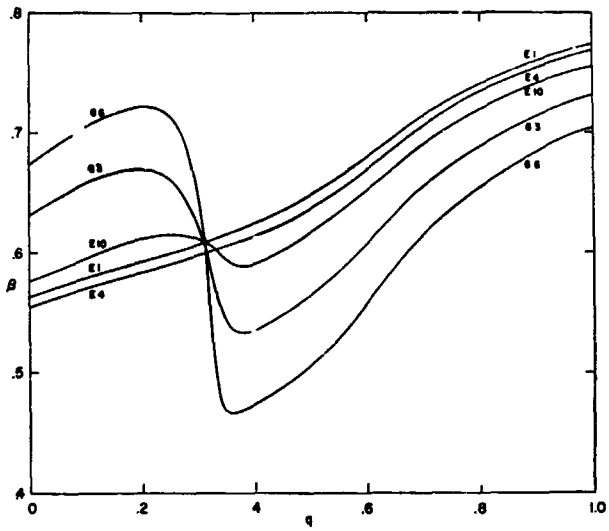

FIGURE 7.—Ratio of gas pressure to total pressure as a function of mass fraction. Curves are labeled with the model numbers.

The effective termination point of the envelope must be taken just outside the shell peak, where U is a minimum on the $U-V$ plane. Now it may be shown generally for a polytrope of any index and constant $\beta=\beta_c$ that $R \sim (T_c/\beta_c\rho_c)^{1/2}$. Eliminating ρ, we have $R \sim (1-\beta_c)^{1/2}/\beta_c T_c$. Thus the expansion may be considered as fundamentally due to the relative increase in radiation pressure, as stated above. Further, the same result can be obtained by examining equation (8). A decrease in β causes expansion by making ϵ_g negative, and an increase causes contraction by making ϵ_g positive. The consequences may be seen by comparing Figures 5–7. During phases of roughly constant β, the change of T will determine the change in R.

If we take the stellar core to be a polytrope, then we may similarly explain the changes of shell radius, r_s (see Tables 1 and 3). By extension, a star with m shell sources may be subdivided into $m+1$ zones whose structure is assumed to be polytropic. Then, approximately, the changes of β and T at a given shell should determine the changes of r at the next outer shell, unless the mass fraction of the shell changes by a drastic amount. Qualitative agreement is found between this picture of evolution and the accurate published results on the evolution of stars of $4M_\odot$ and $15.6M_\odot$ from the initial main sequence through carbon burning (Hayashi, Nishida, and

Sugimoto 1962; Hayashi and Cameron 1962; Hayashi, Hoshi, and Sugimoto 1962).

In this regard we note that the last model before helium burning in a star of $1.3M_\odot$ considered by Schwarzschild and Selberg (1962) had $\beta_s = 0.87$. Since they neglected radiation pressure and used $\beta = 1$ throughout, it might be expected that the radii they derive are too small. Indeed the track of their theoretical models on the H–R diagram deviates leftward of the observed red-giant branch in globular clusters. One reason may be the neglect of varying β in their models; apart from other factors, for a closer agreement with observations β should be explicitly included.

Since the envelope evolves independently of the core (each with a fixed mass), the expansion of the envelope must lower the local density. Since β is also decreasing in the envelope, the temperature near q_s actually does not change very much (see Fig. 6). Beyond the shell, however, it [illegible] considerably, because the temperature gradient is approaching the adiabatic value. This increase of the temperature gradient has two major effects: (1) The semiconvective zone moves steadily inward; by Model G6 it has reached $q = 0.48$. The hydrogen discontinuity grows to $X_2 - X_3 = 0.10$, although $\mu_2/\mu_3 = 0.91$ because the actual hydrogen content is lower at small q. (2). The shell source becomes narrower, on account of the decreasing temperature outside (and the decreasing hydrogen content inside). A curious result, not occurring in stars of lower mass, is that q_s moves slightly inward at first because of the rising temperature inside and the rather broad shell distribution of hydrogen, but thereafter remains stationary as it encounters less and less hydrogen. The total amount of hydrogen depletion (in the shell) is 0.0004, and the maximum local change in X is 0.011 at $q = 0.329$.

In the core, although β_c steadily rises, the central convection persists and recedes only to a roughly constant $q_4 = 0.06$ at the onset of helium burning. Hence convection probably never disappears completely from the center of very massive stars.

Model G6 corresponds to the onset of helium burning. At this point, $L_{He}/L \approx 0.004$ and T_c is 150 million degrees. This value of T_c is almost the same as the corresponding value for a star of $15.6M_\odot$ because of the steep temperature dependence of the energy-generation formula. However, ρ_c is only 270 gm/cm^3, lower by a factor of 10 than in the star of $15.6M_\odot$. But in the heavier star the core mass is four times as large.

The gravitational contraction phase is very short (9×10^3 years), although large changes in the stellar radius take place.

VI. FINAL REMARKS

Although the computed values of the *fractional* luminosities should not be considered exact (since we have neglected in the computations to take account of the radiative flux that is absorbed in the expansion of the envelope), nevertheless Figure 8 shows up a brief peak in the luminosity due to gravitational contraction, whereas the nuclear-energy sources are spread over longer time intervals. Since the total energy available to the star as a result of gravitational contraction is small compared with the nuclear-energy store, it is expected that the time scale of contraction phases will be very short. Indeed, the post–main-sequence age at the onset of helium burning is 4.9 million years, of which 4.8 million are spent burning almost half of the initial hydrogen content.

During this time the interior structure of the star undergoes drastic changes, especially in the

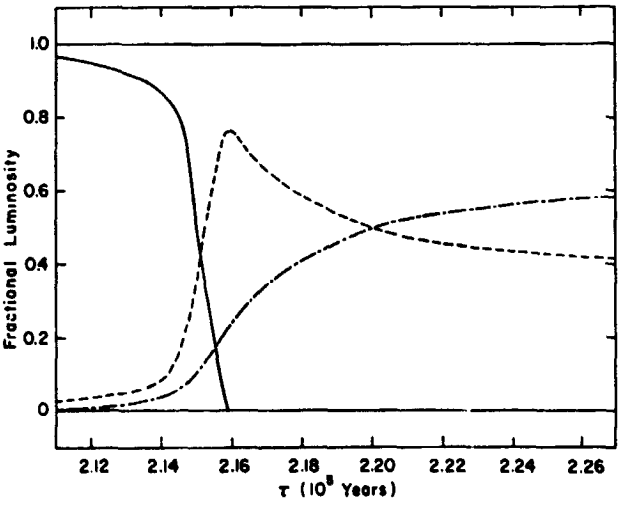

FIGURE 8.—The fraction of the total luminosity contributed by hydrogen burning in the core *(solid curve)*, gravitational contraction in the core *(dashed curve)*, and hydrogen burning in the shell *(dash-dot-curve)* is plotted against the time elapsed since the last model of the hydrogen-burning phase (Model H4 of Paper I).

short (0.1×10^6 years) contraction phase, as shown in Figure 9. One complication not occurring in stars of lower mass may arise from the existence of the semiconvective zone. That is, the inward-moving semiconvection brings hydrogen-enriched material toward the shell source, which is simultaneously moving outward. A hydrogen flare-up might be expected to occur. However, the results of Table 3 show that ΔX is only about 0.1 at the radiative-semiconvective interface. Moreover, from the results on a star of $15.6 M_\odot$ (Hayashi and Cameron 1962; Hayashi, Hoshi, and Sugimoto 1962), the total luminosity is expected to increase little during helium burning, so that the structure of the envelope (and hence of the semiconvective zone) will change very slowly; the outward motion of q_s is also rather slow. Thus the star could probably accommodate quietly the sharp increase in X, despite the narrowness of the shell source. However, it seems unlikely that the inner edge of the semiconvective zone will ever penetrate the shell before the whole envelope becomes convective during the rightward swing of the evolutionary track in the H–R diagram toward red carbon-burning models. We need only worry about possible hydrogen flaring in stars of mass greater than $30 M_\odot$.

The evolution on the theoretical H–R diagram is shown in Figure 10 for the phases considered in this paper. The ages are given in units of 10^4 years. At $\tau = 9.07$ the spectral class becomes B0, and at $\tau = 9.67$ it is B3. The star is expected never to return to the region of O stars during its active life.

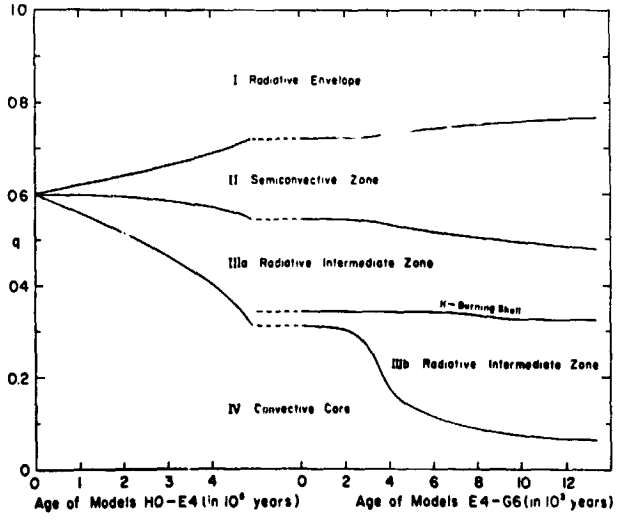

FIGURE 9.—Evolution of the structural zones from the initial main sequence to the onset of helium burning.

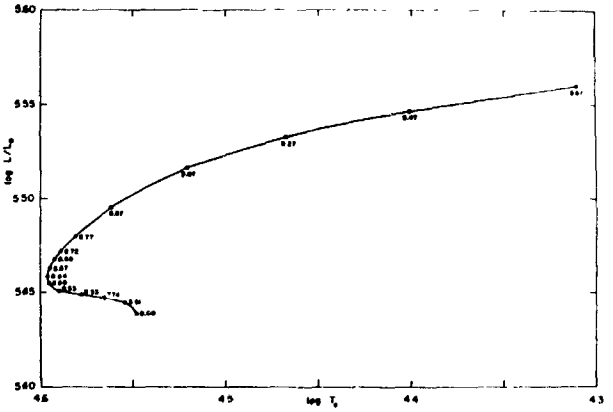

FIGURE 10.—Evolution of a star of 30 M⊙ on a plot of luminosity versus effective temperature, during the phases of hydrogen exhaustion and gravitational contraction. Numbers attached to the models *(filled circles)* represent the age in units of 10^4 years.

REFERENCES

HASELGROVE, C. B., and HOYLE, F. 1956, *M.N.*, **116**, 515.

HAYASHI, C., and CAMERON, R. C. 1962, *Ap. J.*, **136**, 166.

HAYASHI, C., HOSHI, R., and SUGIMOTO, D. 1962, *Prog. Theoret. Phys. Suppl.* (Kyoto), No. 22.

HAYASHI, C., NISHIDA, M., and SUGIMOTO, D. 1962, *Prog. Theoret. Phys.* (Kyoto), **27**, 1233.

HOFMEISTER, E., KIPPENHAHN, R. and WEIGERT, A. 1963, Stellar Evolution Conference (Goddard Institute for Space Studies, New York).

HOYLE, F. 1960, *M.N.*, **120**, 22.

KUSHWAHA, R. S. 1957, *Ap. J.*, **125**, 242.

POLAK, E. J. 1962, *Ap. J.*, **136**, 465.

REEVES, H. 1962, *Stellar Energy Sources* (Goddard Institute for Space Studies, NASA Report).

REIZ, A. 1963, Stellar Evolution Conference (Goddard Institute for Space Studies, New York).

SAKASHITA, S., ÔNO, Y., and HAYASHI, C. 1959, *Prog. Theoret. Phys.* (Kyoto), **21**, 315.

SCHWARZSCHILD, M. 1958, *Structure and Evolution of the Stars* (Princeton, N.J.: Princeton University Press).

SCHWARZSCHILD, M., and HARM, R. 1958, *Ap. J.*, **128**, 348.

SCHWARZSCHILD, M. and SELBERG, H. 1962, *Ap. J.*, **136**, 150.

STOTHERS, R. 1963, *Ap. J.*, **138**, 1074 ("Paper I").

N64-33451

THE RV TAURI POPULATION*

RICHARD STOTHERS

Our understanding of the RV Tauri stars has come mainly from photometric and spectrographic studies based on several tabulations of these stars since 1921.[1–9] Although members of this group are too distant for accurate parallax derterminations, their absolute magnitudes are known through the discovery and identification of some in globular clusters.[5,10] It is the purpose of this paper to analyze the spatial distribution of the RV Tauri stars in the field and to compare properties of these stars with properties of similar stars found in globular clusters.

The data are taken mainly from the *General Catalogue of Variable Stars*[8] (*GCVS*), which lists 92 stars of this class based on criteria that are essentially those of Payne-Gaposchkin, Brenton, and Gaposchkin.[4] RV Tauri stars are supergiants with (1) comparatively stable periodicity of light variation, whose amplitude may reach 3 magnitudes, (2) alternating shallow and deep minima, which occasionally interchange, (3) double-period of 30–150 days, and (4) F to K spectral class, which is earliest near maximum light. From the *GCVS* list we disregard those variables designated RV? and include only stars with periods in the range 39–110 days, since this is roughly the range of RV Tauri stars in globular clusters. Although some types of red variables in the same period range have light curves resembling those of RV Tauri stars, we assume that those variables without known spectra are yellow. In some cases photographic magnitudes were obtained from other sources.[4,6] Since the magnitude of CN Centauri is uncertain at minimum, it has been omitted from the distance determinations. Preston, Krzeminski, Smak, and Williams have shown that UU Herculis and V453 Ophiuchi are RV Tauri stars.[9] Apart from these two variables, their list of RV Tauri stars does not otherwise conflict with assignments given by the *GCVS*, in the period range 39-110 days. We have used their magnitudes and period for V 453 Ophiuchi. The total number of variables whose distances we may determine is 45, of which 25 have known spectra.

Preston *et al.*[9] have defined three groups of RV Tauri stars on spectroscopic criteria: A.—All spectral features indicate type G or K, except that TiO bands may occur during deep light minima. B.—The type based on the Ca II lines differs from that based on the hydrogen lines; strong CN bands occur at and around light minima. C.—The spectrum resembles that group B, except that CN bands never appear. Moreover, the stars in group A are redder than those in groups B and C (which cannot be distinguished photometrically). The RV Tauri stars may be distinguished from the yellow semiregulars on the basis of U,B,V colors and strength of hydrogen emission. At the end of this paper we shall comment on these subdivisions.

The distribution of RV Tauri stars in longitude is far from scraggly, contrary to the results indicated by the smaller numer of stars used in earlier investigations.[7] Indeed, Figure 1 shows a strong concentration of stars in the direction of the galactic center. Their spatial concentration depends on a knowledge of distances, which we may obtain from globular clusters.

In general, RV Tauri stars in globular clusters are specified by the same criteria as those in the field. Small deviations from these criteria have been discussed by Rosino[5] and Joy.[6] Other differences will be pointed out below. Using the mean photographic magnitudes of the nine certain RV Tauri stars in clusters (from the writer's previous paper,[10] hereafter called Paper I), we

*Published in the *Publications of the Astronomical Society of the Pacific*, 76 (449): 98–105, April 1964.

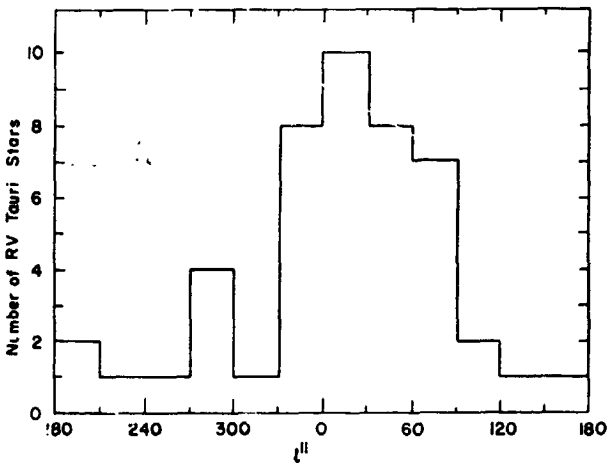

FIGURE 1.—Frequency distribution of the field RV Tauri stars in longitude.

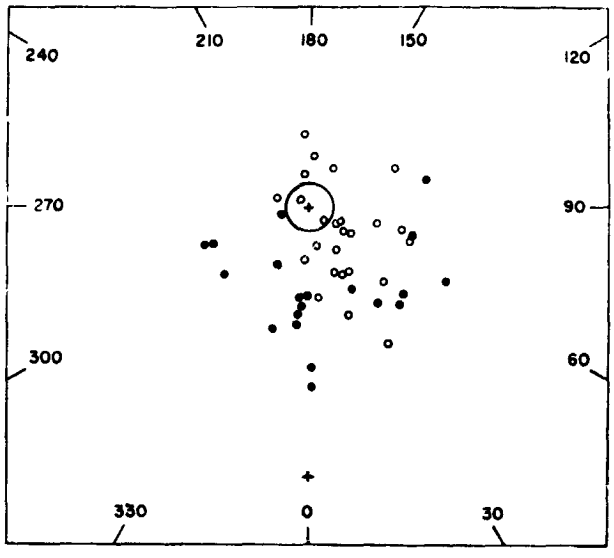

FIGURE 2.—Field RV Tauri stars with known spectra (open circles) and unknown spectra (filled circles) are projected on the galactic plane. The positions of the sun and galactic center are denoted by + signs. The circle around the sun has a radius of 1 kpc.

may obtain a period-luminosity relation, if the distance moduli of the clusters are known. We take the moduli from Hogg's list,[11] where she assumed that $M_{pg}=0.0$ for the RR Lyrae stars. For M 2, M 5, and M 13, we have used the values of M_v of the RR Lyrae stars corrected for reddening listed by Arp[12] and have added C.I. $=+0.1$. For M 22, which closely resembles M 13,[13,14] and for ω Centauri, which has a main sequence turnoff at the same magnitude as M 3[15] (also listed by Arp), we assume analogous values of M_{pg}. For M 56 and NGC 6712 we adopt the mean of all the known values, $M_{pg}=+0.3$. Applying these corrections to Hogg's distance moduli, we obtain absolute magnitudes of the cluster RV Tauri stars. The period-luminosity relation is then $<M_{pg}>=-4.0+0.026P\pm0.36$, where P is in days, in reasonable agreement with previous determinations which depended on indirect or statistical methods.[5,6,7,17,18,19,20,21]

To calculate the distance of the RV Tauri stars in the field, we use

$$<M_{pg}>=<m_{pg}>-10-5\log r-a$$

where r is in kpc and $a=0.7r$ if $|b^{II}|<20°$ or $0.25\csc|b^{II}|$ if $|b^{II}|>20°$. The first formula for extinction is used by Payne-Gaposchkin[16] and also happens to be the mean of extinctions derived for five RV Tauri stars by Kameny.[7]

Figure 2 shows the RV Tauri stars projected on the galactic plane. Variables with known spectra are indicated by open circles, those with unknown spectra by filled circles; the crosses denote the positions of the sun and the galactic center. It is difficult to corroborate the previously suspected[7] groupings near Ophiuchus (30°), Aquila (40°), and Gemini (180°), on the meager data available and the uncertain extinction. Other clumpings at 60° and 75° are also suspect, although the Sagittarius group (0°) is probably real. There is no apparent correlation of period with position in the Galaxy.

Figure 3 shows a vertical cross-section of the Galaxy, where the sun is assumed to lie at 10 kpc from the galactic center. As indicated also by Figures 1 and 2, the number of variables increases in the direction of the galactic center. Their apparent absence at low galactic heights is due to interstellar extinction. The distribution strongly resembles that of the long-period variables with $P<250$ days, that is, intermediate between the distribution of long-period variables with $P>250$ days (Population I) and the distribution of the halo RR Lyrae stars (Population II).[18] The vertical density gradient y, where $\log N=x-y$ (r sin b) and N is the relative number of stars, is 1.1, and the median height $\overline{r \sin b}$ is 0.45 kpc. Both these quantities are similar to those for the long-period variables with $P<250$ days.

Perepelkina suspected that the RV Tauri stars form an intermediate subsystem.[17] Their relatively low radial velocities and latitudes indicate

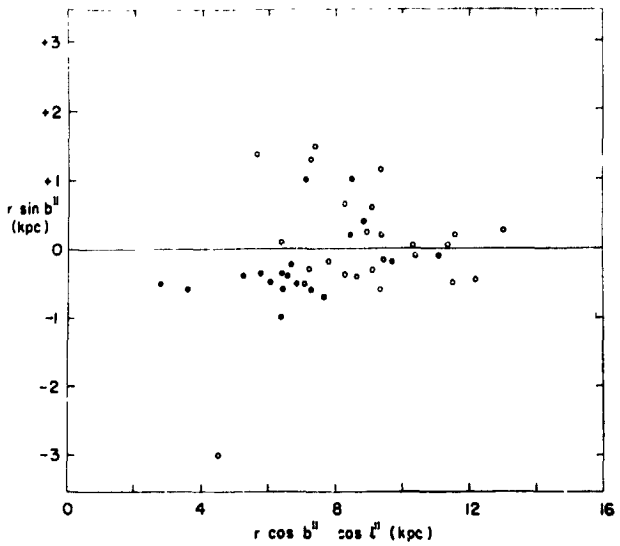

FIGURE 3.—Vertical cross-section of the Galaxy, showing the distribution of field RV Tauri stars on the assumption that the sun lies at 10 kpc from the galactic center. Same symbols as in Figure 2.

a weak Population I, but their excessive blueness (like the W Virginis stars) and discontinuous velocity curves indicate Population II.[7] The yellow semiregulars, however, seem to be real Population II objects.

The general similarity of the RV Tauri stars in globular clusters to those in the field and the approximately equal ratios of number of RV Tauri stars to number of RR Lyrae stars[7] indicate that field and cluster RV Tauri stars belong to the same family. At maximum light the RV Tauri stars are usually the brightest cluster members and are found close to the cluster center (compared with the long-period variables).[10] Therefore, because of the long relaxation times of globular clusters, it seems unlikely that the RV Tauri stars in the field have evaporated from clusters, even apart from the observation that they do not form a halo population.

Besides their spatial distribution, some other differences between the field and cluster variables should be mentioned. While Rosino found no period-spectrum relation for the variables in the field,[8] Paper I showed such a relation for the cluster variables, although the stars seem to be separated chiefly into a 60- and a 90-day group. Kameny[7] found that the short-period RV Tauri stars in the clusters were slightly bluer than those in the field. No very long-period RV Tauri stars have yet been identified in globular clusters. Moreover, in the clusters there is a marked absence of RV Tauri stari stars in the period range 68–87 days. We note in Table I an actual anticorrelation of period frequency with the corresponding field variables. Lastly, we mention that

TABLE I.—*Period Frequencies of the RV Tauri Stars*

P (days)	Globular Clusters		Field	
	RV	All Variables	RV (with Sp.)	RV (all)
28–47	0	1	3	5
48–67	5	7	6	15
68–87	0	2	15	23
88–107	4	13	3	5
>107	0	16	5	24

no RV Tauri stars in globular clusters have light amplitudes exceeding 2 magnitudes, whereas about one-third of the field stars in the same period range have greater amplitudes. All these differences may be due to different ages and chemical compositions.

The results of work by Preston *et al.*[9] indicate that, at least spectroscopically, the RV Tauri stars do not comprise a homogeneous class. Their group A of these stars shows TiO at minimum and resembles kinematically an intermediate (disk) population.[6] Group B is probably also related kinematically to the disk, and we note that it, too, shows the presence of metals in the strong CN bands. The radial velocities of group C stars are very high and suggest a halo population; the absence of CN is also suggestive. We note that the two variables from globular clusters that Preston *et al.* studied probably belong to the "halo" group C; it is interesting that, whereas groups A and B show a wide range in period, the three field variables from group C have periods lying in the "forbidden" range of the clusters.

If the RV Tauri stars plotted on the vertical cross-section of the Galaxy (Fig. 3) are distinguished according to groups, then it appears that groups B and C adhere very well to the above galactic assignments, whereas group A populates

both the disk and the halo. However, it is clear that RV Tauri stars do not really range far enough to separate groups into halo and disk populations. Therefore the suggestion by Preston *et al.* that groups B and C belong to a larger family raises the further speculation that all the groups form really one family. At least this has been indicated by previous work.

In this connection, we note that there is no apparent relation between spectroscopic criteria and shape of light curve or period. Moreover, the colors appear to form a continuous sequence, despite the spectroscopic differences. Although Preston *et al.* could not obtain reliable luminosity classes at the dispersion they used, Rosino's data[5] suggest that the luminosity class falls with increasing period, in agreement with the results on variables in globular clusters.[10] Comparison of the general period-luminosity relations for the variables in globular clusters and those in the field suggests that any difference in the luminosity between the cluster and field RV Tauri stars does not exceed 1 mag. (Paper I, Fig. 11). We believe that the statistical identification of luminosities in the clusters and in the field is sufficient to outline the general spatial distribution of RV Tauri stars, as considered in this paper.

In conclusion, the RV Tauri stars seems to form an intermediate subsystem between Population I and II. Except for the underabundance of metals and the period-frequency anomaly, the RV Tauri stars in globular clusters resemble their counterparts in the field. Perhaps long-period variables in clusters with late integrated spectra should be investigated for RV Tauri behavior; in this connection we note the 105-day variable in NGC 6712 (GA). Certainly the known semiregular and irregular variables with undetermined periods should be checked for periods in the range 68–87 days.

REFERENCES

[1] H. Ludendorff, *A.N.*, **214**, 217, 1921.

[2] H. Ludendorff, in *Handbuch der Astrophysik*, Vol. 6, G. Eberhard, A. Kohlschütter, and H. Ludendorff, eds. (Berlin: Springer 1928), p. 174.

[3] B. P. Gerasimovic, *Harvard Obs. Circ.* No. 341, 1929.

[4] C. H. Payne-Gaposchkin, V. K. Brenton, and S. Gaposchkin, *Harvard Obs. Ann.*, **113**, 1; 1943.

[5] L. Rosino, *Ap. J.*, **113**, 60, 1951.

[6] A. H. Joy, *Ap. J.*, **115**, 25, 1952.

[7] F. E. Kameny, Dissertation, Harvard University, 1956.

[8] B. V. Kukarkin, P. P. Parenago, Yu. I. Efremov, and P. N. Kholopov, *General Catalog of Variable Stars* (Moscow: Academy of Sciences, U.S.S.R. Press, 1958).

[9] G. W. Preston, W. Krzeminski, J. Smak, and J. A. Williams, *Ap. J.*, **137**, 401, 1963.

[10] R. Stothers, *A. J.*, **68**, 242, 1963.

[11] H. S. Hogg, in *Handbuch der Physik*, Vol. 53, S. Flügge, ed. (Berlin: Springer 1959), p. 129.

[12] H. Arp, *Ap. J.* **135**, 971, 1962.

[13] H. C. Arp and W. G. Melbourne, *A. J.*, **64**, 28, 1959.

[14] A. Sandage and G. Wallerstein, *Ap. J.*, **131**, 598, 1960.

[15] E. P. Belserene, *A. J.*, **64**, 58, 1959.

[16] C. H. Payne-Gaposchkin, *Variable Stars and Galactic Structure* (London: Athlone Press, 1954).

[17] E. D. Perepelkina, *Perem. Zvezdy* (*Variable Stars*), **7**, 230, 1950.

[18] P. P. Parenago, *Astr. Zhurnal U.S.S.R.*, **11**, 95, 1934.

[19] A. H. Joy, *Pub. A. S. P.*, **46**, 51, 1934.

[20] W. S. Adams, A. H. Joy, M. L. Humason, and A. M. Brayton, *Ap. J.*, **81**, 187, 1935.

[21] D. McLaughlin, *Pub. Michigan Obs.*, **7**, 57, 1938.

II. CELESTIAL MECHANICS AND GEODESY

LONG-PERIOD CONTRIBUTIONS TO THE DISTURBING FUNCTIONS OF THE EARTH FROM THE SEVENTH, NINTH, AND ELEVENTH ZONAL HARMONICS*

T. L. FELSENTREGER AND W. J. WICKLESS

INTRODUCTION

It is the purpose of this paper to present explicit formulas for the long-period terms due to the seventh, ninth, and eleventh zonal harmonics in the disturbing function of the earth in the case of an artificial earth satellite. The formulas are given for terms of the satellite's orbital elements and the Delaunay variables. G. Giacaglia (1) has given general expressions for the long-period terms due to any of the zonal harmonics, which can be expressed in terms of the orbital elements. The apparent differences between the results of this paper and those in Giacaglia's have been verified as due to the errors in the latter as it appears in the A.J.

The contributions of the long-period terms to the mean motion of the argument of perigee are also given.

THE DISTURBING FUNCTION

The earth's gravitational potential at a distance r from the center of the earth is

$$U=\frac{\mu}{r}\left[1-\sum_{n=2}^{\infty}\left(\frac{R}{r}\right)^{n}J_nP_n\ (\sin\phi)\right],$$

where

$\mu = GM$

G = gravitational constant

M = mass of the earth

R = radius of the earth

J_n = zonal harmonic coefficients ($n+2$, 3,...)

P_n = Legendre polynomials ($n=2$, 3,...)

ϕ = geocentric latitude.

Here, the earth's radius is adopted as the unit of length. The seventh, ninth, and eleventh Legendre polynomials are

$$P_7\ (\sin\phi)=\frac{1}{16}(429\sin^7\phi-693\sin^5\phi+315\sin^3\phi-35\sin\phi)$$

$$P_9\ (\sin\phi)=\frac{1}{128}(12155\sin^9\phi-25740\sin^7\phi+18018\sin^5\phi-4620\sin^3\phi+315\sin\phi)$$

$$P_{11}\ (\sin\phi)=\frac{1}{256}(88179\sin^{11}\phi-230945\sin^9\phi+218790\sin^7\phi-90090\sin^5\phi+15015\sin^3\phi-693\sin\phi).$$

*Published as *Goddard Space Flight Center Document X-547-64-333*, August 1964.

Let

a = semi-major axis of satellite's orbit

e = eccentricity of orbit

i = inclination of orbital plane to equatorial plane

ℓ = mean anomaly

f = true anomaly

g = argument of perigee.

The Delaunay variables L, G, and H are

$$L=\sqrt{\mu a}$$

$$G=L\sqrt{1-e^2}$$

$$H=G\cos i.$$

Use is also made of the relations

$$\sin\phi=\sin i\sin(f+g)$$

$$\frac{a}{r}=\frac{L^2}{G^2}(1+e\cos f).$$

The long-period terms in the expansion of U as a Fourier series in ℓ and g are given by

$$\frac{1}{2\pi}\int_0^{2\pi} U\,d\ell, \qquad \text{(see reference 2)}$$

making use of the relation

$$d\ell=\frac{L}{G}\,\frac{r^2}{a^2}df.$$

Denoting the long-period parts of U_7, U_9, and U_{11} by Δ_7F_{2p}, Δ_9F_{2p}, and $\Delta_{11}F_{2p}$, respectively, we have

$$\Delta_7F_{2p}=-\frac{21\mu^9J_7e\sin i}{16384L^3G^{13}}\left[10\left(5-135\frac{H^2}{G^2}+495\frac{H^4}{G^4}-429\frac{H^6}{G^6}\right)\left(33-30\frac{G^2}{L^2}+5\frac{G^4}{L^4}\right)\sin g\right.$$

$$-15\left(3-69\frac{H^2}{G^2}+209\frac{H^4}{G^4}-143\frac{H^6}{G^6}\right)\left(11-14\frac{G^2}{L^2}+3\frac{G^4}{L^4}\right)\sin 3g$$

$$\left.+33\left(1-15\frac{H^2}{G^2}+27\frac{H^4}{G^4}-13\frac{H^6}{G^6}\right)\left(1-2\frac{G^2}{L^2}+\frac{G^4}{L^4}\right)\sin 5g\right]$$

$$\Delta_9F_{2p}=-\frac{3\mu^{11}J_9e\sin i}{524288L^3G^{17}}\left[210\left(7-308\frac{H^2}{G^2}+2002\frac{H^4}{G^4}-4004\frac{H^6}{G^6}+2431\frac{H^8}{G^8}\right)\times\right.$$

$$\times\left(7-1001\frac{G^2}{L^2}+385\frac{G^4}{L^4}-35\frac{G^6}{L^6}\right)\sin g-10780\left(1-40\frac{H^2}{G^2}+234\frac{H^4}{G^4}-416\frac{H^6}{G^6}+221\frac{H^8}{G^8}\right)\times$$

$$\times\left(39-65\frac{G^2}{L^2}+29\frac{G^4}{L^4}-3\frac{G^6}{L^6}\right)\sin 3g+12012\left(1-32\frac{H^2}{G^2}+146\frac{H^4}{G^4}-200\frac{H^6}{G^6}+85\frac{H^8}{G^8}\right)\times$$

$$\times\left(5-11\frac{G^2}{L^2}+7\frac{G^4}{L^4}-\frac{G^6}{L^6}\right)\sin 5g-2145\left(1-20\frac{H^2}{G^2}+54\frac{H^4}{G^4}-52\frac{H^6}{G^6}+17\frac{H^8}{G^8}\right)\times$$

$$\left.\times\left(1-3\frac{G^2}{L^2}+3\frac{G^4}{L^4}-\frac{G^6}{L^6}\right)\sin 7g\right]$$

$$\Delta_{11}F_{2p}=\frac{11\mu^{13}J_{11}e\sin i}{67108864L^3G^{21}}\Big[126\Big(21-1365\frac{H^2}{G^2}+13650\frac{H^4}{G^4}-46410\frac{H^6}{G^6}+29393\frac{H^8}{G^8}-23933\frac{H^{10}}{G^{10}}\Big)\times$$

$$\times\Big(41423-77292\frac{G^2}{L^2}+45738\frac{G^4}{L^4}-8652\frac{G^6}{L^6}+63\frac{G^8}{L^8}\Big)\sin g$$

$$-163800\Big(1-61\frac{H^2}{G^2}+570\frac{H^4}{G^4}-1802\frac{H^6}{G^6}+2261\frac{H^8}{G^8}-969\frac{H^{10}}{G^{10}}\Big)\times\Big(323-680\frac{G^2}{L^2}+462\frac{G^4}{L^4}-112\frac{G^6}{L^6}+7\frac{G^8}{L^8}\Big)\sin 3g$$

$$+7020\Big(5-265\frac{H^2}{G^2}+2130\frac{H^4}{G^4}-5746\frac{H^6}{G^6}+6137\frac{H^8}{G^8}-2261\frac{H^{10}}{G^{10}}\Big)\times\Big(323-816\frac{G^2}{L^2}+678\frac{G^4}{L^4}-200\frac{G^6}{L^6}+15\frac{G^8}{L^8}\Big)\sin 5g$$

$$-49725\Big(1-41\frac{H^2}{G^2}+250\frac{H^4}{G^4}-514\frac{H^6}{G^6}+437\frac{H^8}{G^8}-133\frac{H^{10}}{G^{10}}\Big)\times\Big(19+60\frac{G^2}{L^2}+66\frac{G^4}{L^4}-28\frac{G^6}{L^6}-3\frac{G^8}{L^8}\Big)\sin 7g$$

$$+20995\Big(1-25\frac{H^2}{G^2}+90\frac{H^4}{G^4}-130\frac{H^6}{G^6}+85\frac{H^8}{G^8}-21\frac{H^{10}}{G^{10}}\Big)\times\Big(1-4\frac{G^2}{L^2}+6\frac{G^4}{L^4}-4\frac{G^6}{L^6}+\frac{G^8}{L^8}\Big)\sin 9g\Big]$$

CONTRIBUTIONS TO dg/dt

Since the Delaunay set of variables is canonical with respect to the Hamiltonian F, which includes Δ_7F_{2p}, Δ_9F_{2p}, and $\Delta_{11}F_{2p}$, we have

$$\frac{dg}{dt}=-\frac{\partial F}{\partial G}\quad\text{(see reference 2).}$$

Therefore, a computation of $\partial(\Delta_iF_{2p})/\partial g(i=7,9,11)$ provides the long-period terms in dg/dt due to the seventh, ninth, and eleventh zonal harmonics.
The results are

$$\frac{\partial(\Delta_7F_{2p})}{\partial G}=\frac{21\mu^9J_7}{16384L^3G^{14}e\sin i}\Big\{10\Big[(\sin^2 i-e^2)\Big(5-135\frac{H^2}{G^2}+495\frac{H^4}{G^4}-429\frac{H^6}{G^6}\Big)\Big(33-30\frac{G^2}{L^2}+5\frac{G^4}{L^4}\Big)$$

$$+e^2\sin^2 i\Big(65-2025\frac{H^2}{G^2}+8415\frac{H^4}{G^4}-8151\frac{H^6}{G^6}\Big)\Big(33-30\frac{G^2}{L^2}+5\frac{G^4}{L^4}\Big)$$

$$+20e^2\sin^2 i\Big(5-135\frac{H^2}{G^2}+495\frac{H^4}{G^4}-429\frac{H^6}{G^6}\Big)\frac{G^2}{L^2}\Big(3-\frac{G^2}{L^2}\Big)\Big]\sin g$$

$$-15\Big[(\sin^2 i-e^2)\Big(3-69\frac{H^2}{G^2}+209\frac{H^4}{G^4}-143\frac{H^6}{G^6}\Big)\Big(11-14\frac{G^2}{L^2}+3\frac{G^4}{L^4}\Big)+e^2\sin^2 i\Big(39-1035\frac{H^2}{G^2}+3553\frac{H^4}{G^4}$$

$$-2717\frac{H^6}{G^6}\Big)\Big(11-14\frac{G^2}{L^2}+3\frac{G^4}{L^4}\Big)+4e^2\sin^2 i\Big(3-69\frac{H^2}{G^2}+209\frac{H^4}{G^4}-143\frac{H^6}{G^6}\Big)\frac{G^2}{L^2}\Big(7-3\frac{G^2}{L^2}\Big)\Big]\sin 3g$$

$$+33\Big[(\sin^2 i-e^2)\Big(1-15\frac{H^2}{G^2}+27\frac{H^4}{G^4}-13\frac{H^6}{G^6}\Big)\Big(1-2\frac{G^2}{L^2}+\frac{G^4}{L^4}\Big)+e^2\sin^2 i\Big(13-225\frac{H^2}{G^2}+459\frac{H^4}{G^4}$$

$$-247\frac{H^6}{G^6}\Big)\Big(1-2\frac{G^2}{L^2}+\frac{G^4}{L^4}\Big)+4e^2\sin^2 i\Big(1-15\frac{H^2}{G^2}+27\frac{H^4}{G^4}-13\frac{H^6}{G^6}\Big)\frac{G^2}{L^2}\Big(1-\frac{G^2}{L^2}\Big)\Big]\sin 5g\Big\}$$

$$\frac{\partial(\Delta_9 F_{2p})}{\partial G}=\frac{3\mu^{11}J_9}{524288L^3G^{18}e\sin i}\Bigg\{210\Bigg[(\sin^2 i-e^2)\left(7-308\frac{H^2}{G^2}+2002\frac{H^4}{G^4}-4004\frac{H^6}{G^6}+2431\frac{H^8}{G^8}\right)$$

$$\times\left(715-1001\frac{G^2}{L^2}+385\frac{G^4}{L^4}-35\frac{G^6}{L^6}\right)+e^2\sin^2 i\left(119-5852\frac{H^2}{G^2}+42042\frac{H^4}{G^4}-92092\frac{H^6}{G^6}+60775\frac{H^8}{G^8}\right)\left(715\right.$$

$$\left.-1001\frac{G^2}{L^2}+385\frac{G^4}{L^4}-35\frac{G^6}{L^6}\right)+14e^2\sin^2 i\left(7-308\frac{H^2}{G^2}+2002\frac{H^4}{G^4}-4004\frac{H^6}{G^6}\right.$$

$$\left.+2431\frac{H^8}{G^8}\right)\frac{G^2}{L^2}\left(143-110\frac{G^2}{L^2}+15\frac{G^4}{L^4}\right)\Bigg]\sin g$$

$$-10780\Bigg[(\sin^2 i-e^2)\left(1-40\frac{H^2}{G^2}+234\frac{H^4}{G^4}-416\frac{H^6}{G^6}+221\frac{H^8}{G^8}\right)\left(39-65\frac{G^2}{L^2}+29\frac{G^4}{L^4}-3\frac{G^6}{L^6}\right)$$

$$+e^2\sin^2 i\left(17-760\frac{H^2}{G^2}+4914\frac{H^4}{G^4}-9568\frac{H^6}{G^6}+5525\frac{H^8}{G^8}\right)\left(39-65\frac{G^2}{L^2}+29\frac{G^4}{L^4}-3\frac{G^6}{L^6}\right)$$

$$+2e^2\sin^2 i\left(1-40\frac{H^2}{G^2}+234\frac{H^4}{G^4}-416\frac{H^6}{G^6}+221\frac{H^8}{G^8}\right)\frac{G^2}{L^2}\left(65-58\frac{G^2}{L^2}+9\frac{G^4}{L^4}\right)\Bigg]\sin 3g$$

$$+12012\Bigg[(\sin^2 i-e^2)\left(1-32\frac{H^2}{G^2}+146\frac{H^4}{G^4}-200\frac{H^6}{G^6}+85\frac{H^8}{G^8}\right)\left(5-11\frac{G^2}{L^2}+7\frac{G^4}{L^4}-\frac{G^6}{L^6}\right)+e^2\sin^2 i\left(17-608\frac{H^2}{G^2}\right.$$

$$\left.+3066\frac{H^4}{G^4}-4600\frac{H^6}{G^6}+2125\frac{H^8}{G^8}\right)\left(5-11\frac{G^2}{L^2}+7\frac{G^4}{L^4}-\frac{G^6}{L^6}\right)+2e^2\sin^2 i\left(1-32\frac{H^2}{G^2}+146\frac{H^4}{G^4}-200\frac{H^6}{G^6}\right.$$

$$\left.+85\frac{H^8}{G^8}\right)\frac{G^2}{L^2}\left(11-14\frac{G^2}{L^2}+3\frac{G^4}{L^4}\right)\Bigg]\sin 5g$$

$$-2145\Bigg[(\sin^2 i-e^2)\left(1-20\frac{H^2}{G^2}+54\frac{H^4}{G^4}-52\frac{H^6}{G^6}+17\frac{H^8}{G^8}\right)\left(1-3\frac{G^2}{L^2}+3\frac{G^4}{L^4}-\frac{G^6}{L^6}\right)+e^2\sin^2 i\left(17-380\frac{H^2}{G^2}\right.$$

$$\left.+1134\frac{H^4}{G^4}-1196\frac{H^6}{G^6}+425\frac{H^8}{G^8}\right)\left(1-3\frac{G^2}{L^2}+3\frac{G^4}{L^4}-\frac{G^6}{L^6}\right)+6e^2\sin^2 i\left(1-20\frac{H^2}{G^2}+54\frac{H^4}{G^4}-52\frac{H^6}{G^6}\right.$$

$$\left.+17\frac{H^8}{G^8}\right)\frac{G^2}{L^2}\left(1-2\frac{G^2}{L^2}+\frac{G^4}{L^4}\right)\Bigg]\sin 7g\Bigg\}$$

$$\frac{\partial(\Delta_{11}F_{2p})}{\partial G}=\frac{11\mu^{13}J_{11}}{67108864L^3G^{22}e\sin i}\Bigg\{126\Bigg[(\sin^2 i-e^2)\left(21-1365\frac{H^2}{G^2}+13650\frac{H^4}{G^4}-46410\frac{H^6}{G^6}+62985\frac{H^8}{G^8}\right.$$

$$\left.-29393\frac{H^{10}}{G^{10}}\right)\left(41423-77292\frac{G^2}{L^2}+45738\frac{G^4}{L^4}-8652\frac{G^6}{L^6}+63\frac{G^8}{L^8}\right)+e^2\sin^2 i\left(441-31395\frac{H^2}{G^2}+341250\frac{H^4}{G^4}\right.$$

$$\left.-1253070\frac{H^6}{G^6}+1826565\frac{H^8}{G^8}-911183\frac{H^{10}}{G^{10}}\right)\times\left(41423-77292\frac{G^2}{L^2}+45738\frac{G^4}{L^4}-8652\frac{G^6}{L^6}+63\frac{G^8}{L^8}\right)$$

$$+72e^2\sin^2 i\left(21-1365\frac{H^2}{G^2}+13650\frac{H^4}{G^4}-46410\frac{H^6}{G^6}+62985\frac{H^8}{G^8}-29393\frac{H^{10}}{G^{10}}\right)\times\frac{G^2}{L^2}\left(2147\right.$$

$$\left.-2541\frac{G^2}{L^2}+721\frac{G^4}{L^4}-7\frac{G^6}{L^6}\right)\Bigg]\sin g$$

$$-163800\left[(\sin^2 i-e^2)\left(1-61\frac{H^2}{G^2}+570\frac{H^4}{G^4}-1802\frac{H^6}{G^6}+2261\frac{H^8}{G^8}-969\frac{H^{10}}{G^{10}}\right)\times\left(323-680\frac{G^2}{L^2}+462\frac{G^4}{L^4}\right.\right.$$
$$\left.-112\frac{G^6}{L^6}+7\frac{G^8}{L^8}\right)+e^2\sin^2 i\left(21-1403\frac{H^2}{G^2}+14250\frac{H^4}{G^4}-48654\frac{H^6}{G^6}+65569\frac{H^8}{G^8}-30039\frac{H^{10}}{G^{10}}\right)$$
$$\times\left(323-680\frac{G^2}{L^2}+462\frac{G^4}{L^4}-112\frac{G^6}{L^6}+7\frac{G^8}{L^8}\right)+8e^2\sin^2 i\left(1-61\frac{H^2}{G^2}+570\frac{H^4}{G^4}-1802\frac{H^6}{G^6}+2261\frac{H^8}{G^8}\right.$$
$$\left.\left.-969\frac{H^{10}}{G^{10}}\right)\times\frac{G^2}{L^2}\left(170-231\frac{G^2}{L^2}+84\frac{G^4}{L^4}-7\frac{G^6}{L^6}\right)\right]\sin 3g$$
$$+7020\left[(\sin^2 i-e^2)\left(5-265\frac{H_2}{G^2}+2130\frac{H^4}{G^4}-5746\frac{H^6}{G^6}+6137\frac{H^8}{G^8}-2261\frac{H^{10}}{G^{10}}\right)\times\left(323-816\frac{G^2}{L^2}+678\frac{G^4}{L^4}\right.\right.$$
$$\left.-200\frac{G^6}{L^6}+15\frac{G^8}{L^8}\right)+e^2\sin^2 i\left(105-6095\frac{H^2}{G^2}+53250\frac{H^4}{G^4}-155142\frac{H^6}{G^6}+177973\frac{H^8}{G^8}-70091\frac{H^{10}}{G^{10}}\right)$$
$$\times\left(323-816\frac{G^2}{L^2}+678\frac{G^4}{L^4}-200\frac{G^6}{L^6}+15\frac{G^8}{L^8}\right)+24e^2\sin^2 i\left(5-265\frac{H^2}{G^2}+2130\frac{H^4}{G^4}-5746\frac{H^6}{G^6}+6137\frac{H^8}{G^8}\right.$$
$$\left.\left.-2261\frac{H^{10}}{G^{10}}\right)\times\frac{G^2}{L^2}\left(68-113\frac{G^2}{L^2}+50\frac{G^4}{L^4}-5\frac{G^6}{L^6}\right)\right]\sin 5g$$
$$-49725\left[(\sin^2 i-e^2)\left(1-41\frac{H^2}{G^2}+250\frac{H^4}{G^4}-514\frac{H^6}{G^6}+437\frac{H^8}{G^8}-133\frac{H^{10}}{G^{10}}\right)\times\left(19-60\frac{G^2}{L^2}+66\frac{G^4}{L^4}-28\frac{G^6}{L^6}+3\frac{G^8}{L^8}\right)\right.$$
$$+e^2\sin^2 i\left(21-943\frac{H^2}{G^2}+6250\frac{H^4}{G^4}-13878\frac{H^6}{G^6}+12673\frac{H^8}{G^8}-4123\frac{H^{10}}{G^{10}}\right)\times\left(19-60\frac{G^2}{L^2}+66\frac{G^4}{L^4}-28\frac{G^6}{L^6}+3\frac{G^8}{L^8}\right)$$
$$\left.+24e^2\sin^2 i\left(1-41\frac{H^2}{G^2}+250\frac{H^4}{G^4}-514\frac{H^6}{G^6}+437\frac{H^8}{G^8}-133\frac{H^{10}}{G^{10}}\right)\times\frac{G^2}{L^2}\left(5-11\frac{G^2}{L^2}+7\frac{G^4}{L^4}-\frac{G^6}{L^6}\right)\right]\sin 7g$$
$$+20995\left[(\sin^2 i-e^2)\left(1-25\frac{H^2}{G^2}+90\frac{H^4}{G^4}-130\frac{H^6}{G^6}+85\frac{H^8}{G^8}-21\frac{H^{10}}{G^{10}}\right)\times\left(1-4\frac{G^2}{L^2}+6\frac{G^4}{L^4}-4\frac{G^6}{L^6}+\frac{G^8}{L^8}\right)\right.$$
$$+e^2\sin^2 i\left(21-575\frac{H^2}{G^2}+2250\frac{H^4}{G^4}-3510\frac{H^6}{G^6}+2465\frac{H^8}{G^8}-651\frac{H^{10}}{G^{10}}\right)\times\left(1-4\frac{G^2}{L^2}+6\frac{G^4}{L^4}-4\frac{G^6}{L^6}+\frac{G^8}{L^8}\right)$$
$$\left.+8e^2\sin^2 i\left(1-25\frac{H^2}{G^2}+90\frac{H^4}{G^4}-130\frac{H^6}{G^6}+85\frac{H^8}{G^8}-21\frac{H^{10}}{G^{10}}\right)\times\frac{G^2}{L^2}\left(1-3\frac{G^2}{L^2}+3\frac{G^4}{L^4}-\frac{G^6}{L^6}\right)\right]\sin 9g\Bigg\}.$$

REFERENCES

1. Giacaglia, Giorgio E. O., "The Influence of High-Order Zonal Harmonics on the Motion of an Artificial Satellite without Drag," Astronom. J. 69(4):303–308, May 1964.
2. Brouwer, D., "Solution of the Problem of Artificial Satellite Theory without Drag," Astronom. J. 64(9): 378–397, November 1959.

NOTES ON VON ZEIPEL'S METHOD*

GIORGIO E. O. GIACAGLIA

1. INTRODUCTION

Since the rediscovery of von Zeipel's method by D. Brouwer (1959) and its successful application to the problem of artificial satellites, many other problems have been solved by that same method, thus proving its great applicability. It is the purpose of these notes to present the general equations of von Zeipel's method and discuss briefly their applicability.

The reduction of the order of a differential canonical system can, in theory, be performed by obtaining, one way or another, integrals of the system. One of them is the Hamiltonian itself when it is time independent. Actually, this integral of the system (physically its "energy"), can describe completely the geometry of the solutions in a phase space of $2n$ dimensions where $2n$ is the order of the system. When this order is 2, then the solution is completely specified and the use of the Hamiltonian reduces it to a first order differential equation which can be integrated by quadrature. The introduction of p integrals in a system of n degrees of freedom ($2n^{th}$ order), reduces it to one of $n-p$ degrees of freedom which can be integrated immediately when $n-p\leq 1$ (where, of course, p cannot be greater than n).

A few comments can be made with respect to the more famous methods of reduction to show their eventual connection with von Zeipel's method.

2. FROM HAMILTON TO VON ZEIPEL

In the discussion that follows only methods that have been used in connection with differential systems describing the motion of a physical system are considered. The presentation does not necessarily follow a chronological order.

Consider then a system of n degrees of freedom given by $2n$ first order canonical equation

$$\dot{x}_j=\frac{\partial H}{\partial y_j} \qquad (j=1, 2, \cdots, n) \qquad (1)$$
$$\dot{y}_j=-\frac{\partial H}{\partial x_j}$$

where the Hamiltonian $H=H(x_1,\ldots,x_n,y_2,\ldots y_n)$ is presumed to be time independent. If this is not the case, the introduction of time as a new canonical coordinate x_{n+1} (the associated momentum being $-H$) always reduces the latter to the former case. The degree of freedom will however increase by one.

A canonical transformation of the variables (x,y) to new variables (x',y') will be, *in this exposition*, equivalent to the problem of finding a generating function $S=S(x',y,t)$ such that

$$y'_j=\frac{\partial S}{\partial x'_j} \qquad (j=1, 2, \cdots, n) \qquad (2)$$
$$x_j=\frac{\partial S}{\partial y_j}.$$

It is easily seen that this is a sufficient condition to satisfy the Jacobi-Poincare relation

$$\sum_{j=1}^{n}(x_j\,dy_j-x'_j\,dy'_j)=dW. \qquad (3)$$

which is valid whether or not S is an explicit function of time. The Hamiltonian of the new system will be equal to that of the old one inasmuch as one is obtained from the other by introducing the transformation of variables expressed by Equations (2) when $\partial S/\partial t=0$.

a. *HAMILTON-JACOBI*—The method introduced by Hamilton and Jacobi consists in obtaining a canonical transformation such that the new

*Published as *Goddard Space Flight Center Document X-547-64-161*, June 1964.

Hamiltonian is identically zero. In such a case, the new variables are all constants.

b. *LINDSTEDT'S METHOD*—Lindstedt's method is a particular application of the Hamilton-Jacobi method for cases where the Hamiltonian is expanded in terms of small parameters. In this particular case the solution gives the coordinates as linear functions of time and the momenta as constants (usually called action angle variables). The comparison with the Hamilton-Jacobi method is purely formal since the method devised by Lindstedt is quite original. Actually, the real difference between von Zeipel's and this method is that Lindstedt does not make use of a generating function.

c. *WHITTAKER'S METHOD* (solution by series). This method obtains n integrals of the system by reducing the Hamiltonian to a function of the products $p_j=x_jy_j(j=1,2,\ldots,n)$. In this case, since

$$\dot{x}_j=\frac{\partial H}{\partial y_j}=\frac{\partial H}{\partial p_j}x_j$$

$$\dot{y}_j=-\frac{\partial H}{\partial x_j}=-\frac{\partial H}{\partial p_j}y_j,$$

it follows that

$$\dot{x}_j\dot{y}_j+x_jy_j=0 \text{ or } p_j=\text{const } (j+1,2,\ldots,n).$$

d. *DELAUNAY'S METHOD*—This method, as Lindstedt's, can be applied only when the Hamiltonian consists of a "zero order" part (the corresponding system having a known solution) and a "disturbing function" that has a small numerical factor. The basic approach of the von Zeipel's method is the same as that of Delaunay's method; however, the latter one makes no use of a generating function and breaks the disturbing function into parts which are treated separately. The Hamiltonian must be constructed after the transformation is performed for each particular part.

A few more techniques could be mentioned but one deserves more attention than all the others. The concept of adiabatic invariants in Quantum Mechanics is quite analogous to the concept of "mean variables" in von Zeipel's method, or to a certain extent to what Whittaker calls Adelphic Integrals.

3. THE VON ZEIPEL'S METHOD (1916)

It has been quite common, after Delaunay, to use the negative of the Hamiltonian. Thus, if $F=-H$ and if $\ell_j(j=1,2,\ldots,n)$ and $L_j(j=1,2,\ldots,n)$ are the coordinates and momenta respectively, then

$$\dot{\ell}_j=-\frac{\partial F}{\partial L_j}$$

$$(j=1, 2, \cdots, n) \qquad (4)$$

$$\dot{L}_j=\frac{\partial F}{\partial \ell_j}.$$

Suppose

$$F=F(\ell,L;\epsilon) \qquad (5)$$

where ϵ is a "small parameter" and ℓ and L indicate the sets $(\ell_1,\ldots,\ell n)$ and $(L_1,\ldots,L_n)$. A canonical transformation involving the parameter ϵ will be given by a generating function

$$S=S(\ell,L^*;\epsilon)$$

such that

$$L_j=\frac{\partial S}{\partial \ell_j}$$

$$(j=1, 2, \cdots, n)$$

$$\ell_j^*=\frac{\partial S}{\partial L_j^*} \qquad (6)$$

where (ℓ^*,L^*) are the new coordinates and momenta. If F^* is the negative of the new Hamiltonian, then we assume

$$F^*(\ell^*,L^*;\epsilon)=F(\ell(\ell^*,L^*;\epsilon),L(\ell^*,L^*;\epsilon);\epsilon) \qquad (7)$$

or, from Equations (6),

$$F^*\left(\frac{\partial S}{\partial L^*},\ L^*;\ \epsilon\right)=F\left(\ell,\frac{\partial S}{\partial L};\ \epsilon\right). \qquad (8)$$

In a more restrictive sense it is assumed that the series

$$\bar{F}=\sum_{k=0}^{N}\epsilon^kF_k(\ell,\ L) \qquad (9)$$

represents the negative of the Hamiltonian to the required degree of precision and converges to $F(\ell,L;\epsilon)$ as $N\to\infty$. From this point $\bar{F}$ is written

as F without danger of confusion. Furthermore, it is assumed that

$$S(\ell, L^*; \epsilon)$$

$$F_k(\ell, L)$$

$$F^*(\ell^*, L^*; \epsilon)$$

are developable in Taylor's series in the neighborhood of $\epsilon=0$, so that the series

$$S=\sum_{k=0}^{\infty}\epsilon^k S_k(\ell, L^*)_{\epsilon=0}$$

$$F_p\left(\ell, \frac{\partial S}{\partial \ell}\right)=\sum_{k=0}^{\infty}\frac{\epsilon^k}{k!}\left(\frac{d^k F_p}{d\epsilon^k}\right)_{\epsilon=0} \tag{10}$$

are convergent for sufficiently small ϵ.

By the conservation property

$$\sum_{k=0}^{\infty}\epsilon^k F_k\left(\ell, \frac{\partial S}{\partial \ell}\right)=\sum_{k=0}^{\infty}\frac{\epsilon^k}{k!}\left(\frac{d^k F^*}{d\epsilon^k}\right)_{\epsilon=0} \tag{11}$$

where it is important to note that $\partial S/\partial \ell$ contains ϵ through Equation (6). Equating the coefficients of like powers in ϵ in both sides of Equation (11) gives a system of partial differential equations in S and F^*. The next step is obtaining this system.

4. DIFFERENTIAL EQUATIONS OF THE VON ZEIPEL'S METHOD

The m^{th} derivative of F_k with respect to ϵ at the point $\epsilon=0$ is obtained as follows.

Consider

$$\frac{dF_k}{d\epsilon}=\sum_{i=1}^{n}\frac{\partial F_k}{\partial L_i}\frac{dL_i}{d\epsilon}=\sum_{i=1}^{n}\frac{\partial F_k}{\partial L_i}\frac{d}{d\epsilon}\left(\frac{\partial S}{\partial \ell_i}\right).$$

Using Equation (10) it follows that

$$\left(\frac{dF_k}{d\epsilon}\right)=\sum_{i=1}^{n}\frac{\partial F_k}{\partial L_i}\frac{d}{d\epsilon}\left\{\sum_{j=0}^{\infty}\epsilon^j\frac{\partial S_j(\ell, L^*)}{\partial \ell_i}\right\}=\sum_{i=1}^{n}\sum_{j=1}^{\infty}j\,\epsilon^{j-1}\frac{\partial F_k}{\partial L_i}\left(\frac{\partial S_j}{\partial \ell_i}\right)_{\epsilon=0}. \tag{12}$$

Let us now compute

$$\frac{d^{m-1}}{d\epsilon^{m-1}}\left(\epsilon^{j-1}\frac{\partial F_k}{\partial L_i}\right)$$

where

$$F_k=F_k\left(\ell, \frac{\partial S}{\partial \ell}\right).$$

Applying Leibniz' formula, this becomes

$$\frac{d^{m-1}}{d\epsilon^{m-1}}\left(\epsilon^{j-1}\frac{\partial F_k}{\partial L_i}\right)=\sum_{\nu=0}^{\min(m-1,\, j-1)}\binom{m-1}{\nu}\frac{d^\nu \epsilon^{j-1}}{d\epsilon^\nu}\frac{d^{m-1-\nu}}{d\epsilon^{m-1-\nu}}\left(\frac{\partial F_k}{\partial L_i}\right).$$

For $\epsilon=0$ the only possible choice is $j<m$. Then

$$\left\{\frac{d^{m-1}}{d\epsilon^{m-1}}\left(\epsilon^{j-1}\frac{\partial F_k}{\partial L_i}\right)\right\}_{\epsilon=0}=\binom{m-1}{j-1}(j-1)!\left\{\frac{d^{m-j}}{d\epsilon^{m-j}}\left(\frac{\partial F_k}{\partial L_i}\right)\right\}_{\epsilon=0}.$$

Now using Equation (12)

$$\left(\frac{d^m F_k}{d\epsilon^m}\right)_{\epsilon=0}=\sum_{i=1}^{n}\sum_{j=1}^{\infty}j\binom{m-1}{j-1}(j-1)!\left\{\frac{d^{m-j}}{d\epsilon^{m-j}}\left(\frac{\partial F_k}{\partial L_i}\right)\right\}_{\epsilon=0}\left(\frac{\partial S_j}{\partial \ell_i}\right)_{\epsilon=0}.$$

It is now desirable to rewrite the above equation as

$$\left(\frac{d^m F_k}{d\epsilon^m}\right)_{\epsilon=0}=\sum_{i_1=1}^{n}\sum_{j_1=1}^{\infty}j_1\frac{(m-1)!}{(m-j_1)!}\left(\frac{\partial S_{j_1}}{\partial \ell_{i_1}}\right)_{\epsilon=0}\left[\frac{d^{m-j_1}}{d\epsilon^{m-j}}\left(\frac{\partial^1 F_k}{\partial L_{i_1}}\right)\right]_{\epsilon=0}. \tag{13}$$

Equation (13) is now applied to find

$$\left[\frac{d^{m-j_1}}{d\epsilon^{m-j_1}}\left(\frac{\partial^1 F_k}{\partial L_{i_1}}\right)\right]_{\epsilon=0}^{\cdot}.$$

The result is

$$\left[\frac{d^{m-j_1}}{d\epsilon^{m-j_1}}\left(\frac{\partial^1 F_k}{\partial L_{i_1}}\right)\right]_{\epsilon=0}^{\cdot}=\sum_{i_2=1}^{n}\sum_{j_2=1}^{\infty}j_2\frac{(m-j_1-1)!}{(m-j_1-j_2)!}\left(\frac{\partial S_{j_2}}{\partial \ell_{i_2}}\right)_{\epsilon=0}\times\left[\frac{d^{m-j_1-j_2}}{d\epsilon^{m-j_1-j_2}}\left(\frac{\partial^2 F_k}{\partial L_{i_1}\partial L_{i_2}}\right)\right]_{\epsilon=0}^{\cdot}$$

The process is repeated up to the point where

$$m-j_1-j_2-\cdots-j_N=0, \tag{14}$$

so that

$$\left[\frac{d^{m-j_1-j_2-\cdots-j_N}}{d\epsilon^{m-j_1-j_2-\cdots-j_N}}\left(\frac{\partial^N F_k}{\partial L_{i_1}\partial L_{i_2}\cdots\partial L_{i_N}}\right)\right]_{\epsilon=0}^{\cdot}=\left(\frac{\partial^N F_k}{\partial L_{i_1}\cdots\partial L_{i_N}}\right)_{\epsilon=0}^{\cdot}.$$

Substituting these successive derivatives into Equation (13), it follows that

$$\left(\frac{d^m F_k}{d\epsilon^m}\right)_{\epsilon=0}^{\cdot}=\sum_{i_1=1}^{n}\sum_{j_1=1}^{\infty}j_1\frac{(m-1)!}{(m-j_1)!}\left(\frac{\partial S_{j_1}}{\partial \ell_{i_1}}\right)_{\epsilon=0}\times\sum_{i_2=1}^{n}\sum_{j_2=1}^{\infty}j_2\frac{(m-j_1-1)!}{(m-j_1-j_2)!}\left(\frac{\partial S_{j_2}}{\partial \ell_{i_2}}\right)_{\epsilon=0}$$

$$\times\sum_{i_3=1}^{n}\sum_{j_3=1}^{\infty}j_3\frac{(m-j_1-j_2-1)!}{(m-j_1-j_2-j_3)!}\left(\frac{\partial S_{j_3}}{\partial \ell_{i_3}}\right)_{\epsilon=0}\times\cdots\times\sum_{i_N=1}^{n}\sum_{j_N=1}^{\infty}j_N\frac{(m-j_1-j_2-\cdots-j_{N-1}-1)!}{(m-j_1-j_2-\cdots-j_N)!}\left(\frac{\partial S_{j_N}}{\partial \ell_{i_N}}\right)_{\epsilon=0}$$

$$\times\left(\frac{\partial^N F_k}{\partial L_{i_1}\partial L_{i_2}\cdots\partial L_{i_N}}\right)_{\epsilon=0}^{\cdot}.$$

The numerical factors are reduced to

$$j_1 j_2\cdots j_N\frac{m!}{m(m-j_1)(m-j_1-j_2)\cdots(m-j_1-j_2-\cdots-j_{N-1})}\equiv m!\,C(m;j_1,j_2,\cdots,j_N)$$

and the second summation does not run in general up to infinity but to a limit given by condition (14). Thus the above relation becomes

$$\left(\frac{d^m F_k}{d\epsilon^m}\right)_{\epsilon=0}^{\cdot}=\sum_{(m)}\prod_{p=1}^{N}\left(\sum_{i_p=1}^{n}\right)m!\,C(m;j_1,\cdots,j_N)\prod_{p=1}^{N}\left(\frac{\partial S_{j_p}}{\partial \ell_{i_p}}\right)_{\epsilon=0}\left(\frac{\partial^N F_k}{\partial L_{i_1}\cdots\partial L_{i_N}}\right)_{\epsilon=0}^{\cdot} \tag{15}$$

where $\sum_{(m)}$ stands for summation over all possible positive integers j_p whose sum is m (according to Equation (14)), and the first product $\prod_{p=1}^{N}$ refers to the summation signs $\sum_{i_p=1}^{n}$. There are n of these integers. Equation (15) will be valid even for $m=0$ with the definitions

$$\frac{d^0 F_k}{d\epsilon^0}\equiv F_k$$

and

$$C(0;-)\equiv 1.$$

From Equations (10) and (11) it follows that

$$F=\sum_{k=0}^{\infty}\epsilon^k F_k(\ell, L)=\sum_{k=0}^{\infty}\epsilon^k\sum_{m=0}^{\infty}\frac{\epsilon^m}{m!}\left(\frac{d^m F_k}{d\epsilon^m}\right)_{\epsilon=0}=\sum_{k=0}^{\infty}\sum_{m=0}^{\infty}\frac{\epsilon^{m+k}}{m!}\left(\frac{d^m F_k}{d\epsilon^m}\right)_{\epsilon=0}=\sum_{\nu=0}^{\infty}\sum_{m=0}^{\nu}\frac{\epsilon_\nu}{m!}\left(\frac{d^m F_{\nu-m}}{d\epsilon^m}\right)_{\epsilon=0}.$$

The substitution of these results into Equation (14) leads to

$$F=\sum_{\nu=0}^{\infty}\sum_{m=0}^{\nu}\sum_{(m)}\prod_{p=1}^{N}\left(\sum_{i_p=1}^{n}\right)C(m; j_1, \cdots, j_N)\prod_{p=1}^{N}\left(\frac{\partial S_{j_p}}{\partial \ell_{i_p}}\right)_{\epsilon=0}\left(\frac{\partial^N F_{\nu-m}}{\partial L_{i_1}\cdots\partial L_{i_N}}\right)_{\epsilon=0}\epsilon^\nu. \tag{16}$$

In a complete similar way, if

$$F^*=\sum_{k=0}^{\infty}\epsilon^k F_k^*\left(\frac{\partial S}{\partial L^*}, L^*\right),$$

then

$$F^*=\sum_{\nu=0}^{\infty}\sum_{m=0}^{\nu}\sum_{(m)}\prod_{p=1}^{N}\left(\sum_{i_p=1}^{n}\right)C(m; j_1, \cdots, j_N)\prod_{p=1}^{N}\left(\frac{\partial S_{i_p}}{\partial L_{i_p}^*}\right)_{\epsilon=0}\left(\frac{\partial^N F_{\nu-m}^*}{\partial \ell_{i_1}^*\cdots\partial \ell_{i_N}^*}\right)_{\epsilon=0}\epsilon^\nu. \tag{17}$$

It is important to note that in Equation (16), $\epsilon=0$ is equivalent to $L_r=\partial S_0/\partial \ell_r (r=1,2,\cdots,n)$, and in Equation (17) $\epsilon=0$ is equivalent to $\ell_r^*=\partial S_0/\partial L_r^* (r=1,2,\cdots,n)$, according to Equation (10). The equality of factors of the same power of ϵ in Equations (16) and (17) gives the partial differential equations for the von Zeipel's method

$$\sum_{m=0}^{\nu}\sum_{(m)}\prod_{p=1}^{N}\left(\sum_{i_p=1}^{n}\right)C(m; j_1, \cdots, j_N)\prod_{p=1}^{N}\left\{\frac{\partial S_{j_p}}{\partial \ell_{i_p}}\left(\frac{\partial^N F_{\nu-m}}{\partial L_{i_p}\cdots\partial L_{i_N}}\right)+-\frac{S\partial_{j_p}}{\partial L_{i_p}^*}\left(\frac{\partial^N F_{\nu-m}}{\partial \ell_{i_1}^*\cdots\partial \ell_{i_N}^*}\right)\right\}_{\epsilon=0}=0 \tag{18}$$

for $\nu=0, 1, 2, \cdots$.

For instance, Equation (18) gives:

$\underline{\nu=0}$

$$F_0\left(\ell, \frac{\partial S_0}{\partial \ell}\right)=F_0^*\left(\frac{\partial S_0}{\partial L^*}, L^*\right) \tag{19}$$

$\underline{\nu=1}$

$$F_1\left(\ell, \frac{\partial S_0}{\partial \ell}\right)+\sum_{i=1}^{n}\left(\frac{\partial S_1}{\partial \ell_i}\frac{\partial F_0}{\partial L_i}\right)_{L_i=\frac{\partial S_0}{\partial \ell_i}}=F_1^*\left(\frac{\partial S_0}{\partial L^*}, L^*\right)+\sum_{i=1}^{n}\left(\frac{\partial S_1}{\partial L_i^*}\frac{\partial F_0^*}{\partial \ell_i^*}\right)_{\ell_i^*=\frac{\partial S_0^*}{\partial L_i^*}} \tag{20}$$

$\underline{\nu=2}$

$$F_2\left(\ell, \frac{\partial S_0}{\partial \ell}\right)+\sum_{i=1}^{n}\left(\frac{\partial S_1}{\partial \ell_i}\frac{\partial F_1}{\partial L_i}\right)_{L_1=\frac{\partial S_0}{\partial \ell_i}}+\sum_{i=1}^{n}\left(\frac{\partial S_2}{\partial \ell_i}\frac{\partial F_0}{\partial L_i}\right)_{L_i=\frac{\partial S_0}{\partial \ell_i}}+\frac{1}{2}\sum_{i,\,j=1}^{n}\left(\frac{\partial S_1}{\partial \ell_i}\frac{\partial S_1}{\partial \ell_j}\frac{\partial^2 F_0}{\partial L_i \partial L_j}\right)_{L_k=\frac{\partial S_0}{\partial \ell_k}}$$

$$=F_2^*\left(\frac{\partial S_0}{\partial L^*}, L^*\right)+\sum_{i=1}^{n}\left(\frac{\partial S_1}{\partial L_i^*}\frac{\partial F_1^*}{\partial \ell_i^*}\right)_{\ell_i^*=\frac{\partial S_0}{\partial L_i^*}}+\sum_{i=1}^{n}\left(\frac{\partial S_2}{\partial L_i^*}\frac{\partial F_0^*}{\partial \ell_i^*}\right)_{\ell_i^*=\frac{\partial S_0}{\partial L_i^*}}+\frac{1}{2}\sum_{i,\,j=1}^{n}\left(\frac{\partial S_1}{\partial L_i^*}\frac{\partial S_1}{\partial L_j^*}\frac{\partial^2 F_0^*}{\partial \ell_i^* \partial \ell_j^*}\right)_{\ell_k^*=\frac{\partial S_0}{\partial L_k^*}} \tag{21}$$

$\nu=3$

$$F_3\left(\ell,\frac{\partial S_0}{\partial \ell}\right)+\sum_{i=1}^{n}\left(\frac{\partial S_1}{\partial \ell_i}\frac{\partial F_2}{\partial L_i}\right)_{L_i=\frac{\partial S_0}{\partial \ell_i}}+\sum_{i=1}^{n}\left(\frac{\partial S_2}{\partial \ell_i}\frac{\partial F_1}{\partial L_i}\right)_{L_i=\frac{\partial S_0}{\partial \ell_i}}+\sum_{i,\,j=1}^{n}\frac{1}{2}\left(\frac{\partial S_1}{\partial \ell_i}\frac{\partial S_1}{\partial \ell_j}\frac{\partial^2 F_1}{\partial L_i \partial L_j}\right)_{L_k=\frac{\partial S_0}{\partial \ell_k}}+$$

$$+\sum_{i,\,j,\,k=1}^{n}\frac{1}{6}\left(\frac{\partial S_1}{\partial \ell_i}\frac{\partial S_1}{\partial \ell_j}\frac{\partial S_1}{\partial \ell_k}\frac{\partial^3 F_0}{\partial L_i \partial L_j \partial L_k}\right)_{L_p=\frac{\partial S_0}{\partial \ell_p}}+\sum_{i,\,j=1}^{n}\left(\frac{\partial S_1}{\partial \ell_i}\frac{\partial S_2}{\partial \ell_j}\frac{\partial^2 F_0}{\partial L_i \partial L_j}\right)_{L_k=\frac{\partial S_0}{\partial \ell_k}}+\sum_{i=1}^{n}\left(\frac{\partial S_3}{\partial \ell_i}\frac{\partial F_0}{\partial L_i}\right)_{L_i=\frac{\partial S_0}{\partial \ell_i}}$$

$$=F_3^*\left(\frac{\partial S_0}{\partial L^*},L^*\right)+\sum_{i=1}^{n}\left(\frac{\partial S_1}{\partial L_i^*}\frac{\partial F_2^*}{\partial \ell_i^*}\right)_{\ell_i^*=\frac{\partial S_0}{\partial L_i^*}}+\sum_{i=1}^{n}\left(\frac{\partial S_2}{\partial L_i^*}\frac{\partial F_1^*}{\partial \ell_i^*}\right)_{\ell_i^*=\frac{\partial S_0}{\partial L_i^*}}+\sum_{i,\,j=1}^{n}\frac{1}{2}\left(\frac{\partial S_1}{\partial L_i^*}\frac{\partial S_1}{\partial L_j^*}\frac{\partial^2 F_1^*}{\partial \ell_i^* \partial \ell_j^*}\right)_{\ell_k^*=\frac{\partial S_0}{\partial L_k^*}}$$

$$+\sum_{i,\,j,\,k=1}^{n}\frac{1}{6}\left(\frac{\partial S_1}{\partial L_i^*}\frac{\partial S_1}{\partial L_j^*}\frac{\partial S_1}{\partial L_k^*}\frac{\partial^3 F_0^*}{\partial \ell_i^* \partial \ell_j^* \partial \ell_k^*}\right)_{\ell_p^*=\frac{\partial S_0}{\partial L_p^*}}+\sum_{i,\,j=1}^{n}\left(\frac{\partial S_1}{\partial L_i^*}\frac{\partial S_2}{\partial L_j^*}\frac{\partial F_0^*}{\partial \ell_i^* \partial \ell_j^*}\right)_{\ell_k^*=\frac{\partial S_0}{\partial L_k^*}}$$

$$+\sum_{i=1}^{n}\left(\frac{\partial S_2}{\partial L_i^*}\frac{\partial F_0^*}{\partial \ell_i^*}\right)_{\ell_i^*=\frac{\partial S_0}{\partial L_i^*}} \tag{22}$$

where use has been made of the coefficients

$C(1;\,1)=1$
$C(2;\,2)=1 \quad C(2;\,1,\,1)=\frac{1}{2}$
$C(3;\,3)=1 \quad C(3;\,2,\,1)=\frac{2}{3} \quad C(3;\,1,\,2)=\frac{1}{3} \quad C(3;\,1,\,1,\,1)=\frac{1}{6}.$

5. ELIMINATION OF VARIABLES

Since the solution of the system is known where F is reduced to F_0, the problem is to eliminate variables which are not present in F_0. Suppose a canonical transformation is found in such a way that p of the n coordinates ($p\leq n$) have been eliminated from the Hamiltonian, that is

$$F^*=F^*(\ell_{p+1}^*,\cdots,\ell_n,L_1^*,L_2^*,\cdots,L_n^*). \tag{23}$$

The equations of motion then yield

$$L_k^*=C_k(\text{const.}) \qquad (k=1,2,\cdots,p). \tag{24}$$

If these constants are replaced in F^*, then

$$F^*=F^*(\ell_{p+1}^*,\cdots,\ell_n^*,C_1,C_2,\cdots,C_p,L_{p+1}^*,\cdots,L_n^*)$$

and the problem is reduced to one of $n-p$ degrees of freedom.

a. If $p=n$, the problem is completely solved, since

$$L_k^*=C_k \qquad (k=1,2,\cdots,n)$$

and

$$\ell_k^*=\omega_k(C_1,\cdots,C_n)t+\ell_k^*(0). \qquad (k=1,2,\cdots,n)$$

b. If $p=n-1$, the problem is integrable by quadrature. In fact,

$$L_k^* = C_k \qquad (k=1,2,\cdots,n-1)$$

$$\dot{L}_n^* = \frac{\partial F^*}{\partial \ell_n^*} = \Lambda(C_1, C_2, \cdots, C_{n-1}; L_n^*, \ell_n^*)$$

$$\dot{\ell}_n^* = -\frac{\partial F^*}{\partial L_n^*} = \lambda_n'(C_1, C_2, \cdots, C_{n-1}; L_n^*, \ell_n^*).$$

Since

$$F^*(C_1,\cdots,C_{n-1}; \ell_n^*, L_n^*) = C = \text{const.},$$

then

$$L_n^* = L_n^*(C, C_1, \cdots, C_{n-1}; \ell_n^*)$$

and therefore

$$\dot{\ell}_n^* = \lambda_n(C, C_1, \cdots, C_{n-1}; \ell_n^*)$$

and

$$t - t_0 = \int_{\ell_{n(0)}^*}^{\ell_n^*} \frac{d\zeta}{\lambda_n(C, C_1, \cdots, C_{n-1}; \zeta)}$$

The coordinate ℓ_n^* becomes a known function of time as well as L_n^*.

Therefore, the equations

$$\dot{\ell}_k^* = -\frac{\partial F^*}{\partial L_k^*} = \lambda_k\Big(C_1, C_2, \cdots, C_{n-1}; L_n^*(t), \ell_n^*(t)\Big) (k=1, 2, \cdots, n-1)$$

can be integrated by quadrature.

The von Zeipel's method consists in the elimination of some of the coordinates (angular variables) and the reduction of the problem to case (b) and possibly (a). The adaptability of this method is based on a set of hypotheses which are listed below in Roman numerals.

(I) The new and old corresponding variables differ by a quantity at least of the first order, i.e.

$$\ell_i' - \ell_i = 0(\epsilon)$$

$$(i=1, 2, \cdots, n)$$

$$L_i^* - L_i = 0(\epsilon).$$

This automatically fixes S_0 to correspond to the identity transformation since for $\epsilon=0$, the above conditions give

$$\ell_i^* \equiv \ell_i$$

$$(i=1, 2, \cdots, n)$$

$$L_i^* \equiv L_i.$$

Therefore

$$S_0 = \sum_{i=1}^{n} \ell_i L_i^*. \tag{25}$$

If expression (25) is substituted into Equations (19), (20), (21) and (22), then

$\nu=0$

$$F_0(\ell, L^*)=F_0^*(\ell, L^*) \tag{26}$$

$\nu=1$

$$F_1(\ell, L^*)+\sum_{i=1}^{n}\left(\frac{\partial S_1}{\partial \ell_i}\right)_{L_i=L_i^*}\frac{\partial F_0}{\partial L_i^*}=F_1^*(\ell, L^*)+\sum_{i=1}^{n}\left(\frac{\partial S_1}{\partial L_i^*}\right)_{\ell_i^*=\ell_i}\frac{\partial F_0^*}{\partial \ell_i} \tag{27}$$

$\nu=2$

$$F_2(\ell, L^*)+\sum_{i=1}^{n}\left(\frac{\partial S_i}{\partial \ell_i}\right)_{L_i=L_i^*}\frac{\partial F_i}{\partial L_i^*}+\sum_{i=1}^{n}\left(\frac{\partial S_2}{\partial \ell_i}\right)_{L_i=L_i^*}\frac{\partial F_0}{\partial L_i^*}+\frac{1}{2}\sum_{i,\,j=1}^{n}\left(\frac{\partial S_1}{\partial \ell_i}\frac{\partial S_1}{\partial \ell_j}\right)_{L_k=L_k^*}\frac{\partial^2 F_0}{\partial L_i^*\partial L_j^*}=F_2^*(\ell, L^*)$$

$$+\sum_{i=1}^{n}\left(\frac{\partial S_1}{\partial L_i^*}\right)_{\ell_i^*=\ell_i}\frac{\partial F_1^*}{\partial \ell_i^*}+\sum_{i=1}^{n}\left(\frac{\partial S_2}{\partial L_i^*}\right)_{\ell_i^*=\ell_i}\frac{\partial F_0^*}{\partial \ell_i}+\frac{1}{2}\sum_{i,\,j=1}^{n}\left(\frac{\partial S_1}{\partial L_i^*}\frac{\partial S_1}{\partial L_j^*}\right)_{\ell_k^*=\ell_k}\frac{\partial^2 F_0^*}{\partial \ell_i\,\partial \ell_j}. \tag{28}$$

and similarly for Equation (22).

It is seen that $S_k(L^*, \ell)$ and $F_k^*(L^*, \ell)$ are unknown functions. In order to perform a particular solution toward the elimination of certain angular variables in F^* we impose conditions (which are usually suitable in Celestial Mechanics) on the functions S_k and F_k^*. They are

II) $F_k^*(L^*, \ell)$ does not depend on $\ell_i(i=1, 2,\cdots,p\leq n)$ for any $k\geq 0$.

III) $S_k(L^*, \ell)$ only depends on the $\ell_i(i=1,2,\cdots,n)$ through trigonometric functions, for any $k>0$. This avoids "secular perturbations" in the momenta L_j, or in other words differences

$$L_j-L_j^*=\frac{\partial(S-S_0)}{\partial \ell_j}$$

are periodic functions of the $\ell_k(k=1, 2,\cdots,n)$.

The application of these conditions, together with the obvious fact that F_0 does not depend on angular variables $\ell_i(i=1,2,\cdots,p\leq n)$ which are to be eliminated, yields the relations

$$F_0(\ell_{p+1},\cdots, \ell_n, L_1^*,\cdots,L_n^*)=F_0^*(\ell_{p+1},\cdots\ell_n,L_1^*\cdots,L_n^*) \tag{29}$$

$$F_{1s}=F_1^*$$

$$F_{1p}+\sum_{i=1}^{n}\left(\frac{\partial S_1}{\partial \ell_i}\right)_{L_i=L_i^*}\frac{\partial F_0}{\partial L_i}=\sum_{i=p+1}^{n}\left(\frac{\partial S_1}{\partial L_i^*}\right)_{\ell_i^*=\ell_i}\frac{\partial F_0^*}{\partial \ell_i} \tag{30}$$

$$F_{2s}+P_{2s}=F_2^*+P_{2s}^*$$

$$F_{2p}+P_{2p}+\sum_{i=1}^{n}\left(\frac{\partial S_2}{\partial \ell_i}\right)_{L_i=L_i^*}\frac{\partial F_0}{\partial L_i^*}=P_{2p}^*+\sum_{i=p+1}^{n}\left(\frac{\partial S_2}{\partial L_i}\right)_{\ell_i^*=\ell_i}\frac{\partial F_0^*}{\partial \ell_i} \tag{31}$$

and so forth. The functions F_{1s} and F_{1p}, F_{2s} and F_{2p}, P_{2s} and P_{2p}, P_{2s}^* and P_{2p}^* are the portions of F_1, F_2, P_2 and P_2^* which are respectively independent of and dependent on the $\ell_i(i=1,2,\cdots,p)$, and where

$$P_2=\sum_{i=1}^{n}\left(\frac{\partial S_1}{\partial \ell_i}\right)_{L_i=L_i^*}\frac{\partial F_1}{\partial L^*}+\frac{1}{2}\sum_{i,\,j=1}^{n}\left(\frac{\partial S_1}{\partial \ell_i}\frac{\partial S_1}{\partial \ell_j}\right)_{L_k=L_k^*}\frac{\partial^2 F_0}{\partial L_i^*\partial L_j^*}$$

$$P_2^*=\sum_{i=p+1}^{n}\left(\frac{\partial S_1}{\partial L_i^*}\right)_{\ell_i^*=\ell_i}\frac{\partial F_1^*}{\partial \ell_i^*}+\frac{1}{2}\sum_{i,\,j=p+1}^{n}\left(\frac{\partial S_1}{\partial L_i^*}\frac{\partial S_1}{\partial L_j^*}\right)_{\ell_k^*=\ell_k}\frac{\partial^2 F_0^*}{\partial \ell_i\partial \ell_j}. \tag{32}$$

In the usual problems of Celestial Mechanics F_0 does not depend on any angular variable so that the Equations (30), (31), (32) and the corresponding equations for higher order are much simplified. Thus, the additional hypotheses will be considered.

IV) F_0 and thus F_0^* depend only on the momenta L_i^*

V) The angular variables ℓ_i $(i=1,2,\cdots,m)$ corresponding to momenta $L_i(i=1,2,\cdots,m)$ that are present in F_0 have been eliminated to the k^{th} order.

The next problem is the possibility of elimination of angular variables whose conjugate momenta are not present in F_0. At this stage the Hamiltonian of the system is

$$F^*=F_0^*(L_1^*,\cdots,L_m^*)+F_1^*(\ell_{m+1},\cdots,\ell_n,L_1^*,\cdots,L_n^*)+\cdots+F_k^*(\ell_{m+1},\cdots,\ell_n,\cdots,L_n^*) \tag{33}$$

where

$$L_j^*=C_j=\text{const}(j=1,2,\cdots,m),$$

and the old and new variables are related by

$$\begin{aligned} L_j-L_j^*&=\frac{\partial S_1}{\partial \ell_j}+\frac{\partial S_2}{\partial \ell_j}+\cdots+\frac{\partial S_K}{\partial \ell_j} \\ \ell_j^*-\ell_j&=\frac{\partial S_1}{\partial L_j^*}+\frac{\partial S_2}{\partial L_j^*}+\cdots+\frac{\partial S_K}{\partial L_j^*}. \end{aligned} \qquad (j=1,2,\cdots,n) \tag{34}$$

Assume a new canonical transformation from the variables $(\ell_{m+1}^*,\cdots,\ell_n^*,L_{m+1}^*,\cdots,L_n^*)$ to the variables $(\ell_{m+1}^{**},\cdots,\ell_n^{**},L_{m+1}^{**},\cdots,L_n^{**})$ and let

$$S^*=S^*(\ell_{m+1}^*,\cdots,\ell_n^*,L_{m+1}^{**},\cdots,L_n^{**}) \tag{35}$$

be its generating function. Then, since $L_j^*=C_j=\text{const}$ $(j=1,2,\cdots,m)$,

$$F_0^*(L_1^{**},\cdots,L_m^{**})=F_0^{**}(L_1^{**},\cdots,L_m^{**})=\text{const } L_k^{**}=L_k^*=C_k=\text{const } (k=1,2,\cdots,m) \tag{36}$$

$$F_1^*(\ell_{m+1}^*,\cdots,\ell_n^*;C_1,C_2,\cdots,C_m,L_{m+1}^{**},\cdots,L_n^{**})=F_1^{**}(\ell_{m+1}^*,\cdots,\ell_n^*;L_{m+1}^{**},\ldots,L_n^{**}). \tag{37}$$

The last equation implies that the elimination of further variables is possible if and only if F_1^* does not depend on them. For in this case

$$F_1^*(\ell_{m+p+1}^*,\cdots,\ell_n^*,C_1,C_2,\cdots,C_n,L_{m+1}^{**},\cdots,L_n^{**})=F_1^{**}(\ell_{m+p+1}^*,\cdots,\ell_n^*;L_{m+1}^{**},\cdots,L_n^{**})$$

and

$$\begin{aligned} F_2^*(\ell_{m+1}^*,\cdots,\ell_n^*;L_{m+1}^{**},\cdots,L_n^{**})+\sum_{i=m+1}^{n}\frac{\partial S_1^*}{\partial \ell_i^*}\frac{\partial F_1^*}{\partial L_i^{**}} \\ =F_2^{**}(\ell_{m+p+1}^*,\cdots,\ell_n^*;L_{m+1}^{**},\cdots,L_n^{**})+\sum_{i=m+p+1}^{n}\frac{\partial S_1^*}{\partial L_i^{**}}\frac{\partial F_1^{**}}{\partial \ell_i^*}. \end{aligned} \tag{38}$$

which defines S_1^*. It is important to note that in such a case S_1^* will be defined by an equation involving *2nd order* terms; these terms are therefore necessary to obtain *first order* "perturbations." This fact is exactly what happens in Brouwer's theory on artificial satellites (1959), where

a) The elimination of g^* is possible because F_1^* is independent of this variable.

b) The development for long period perturbations (those of argument g^*) needs the evaluation of 2nd order terms.

This type of reasoning can be carried on up to any order in exactly the same way. It may then happen that the elimination of a certain angular variable by obtaining S_1^* requires the evaluation of terms of the kth order.

However if F_1^* depends on the angular variables to be eliminated the problem cannot be solved unless it happens that the remaining system has one degree of freedom. For example, this is the case of the perturbations on the motion of an artificial satellite by the moon.

6. SMALL DIVISORS

The case of critical inclination for the theory of artificial satellites of an oblate planet for which P_2 is the dominant zonal harmonic and $J_4 \neq -J_2^2$, is a well known example of the problem of small divisors. Here, only a particular aspect of the question is dealt with. Consider the solution of Equation (30) in the usual case where F_0^* does not depend on the ℓ_i. The characteristic associated system is

$$\frac{d\ell_1}{\dfrac{\partial F_0}{\partial L_1^*}} = \frac{d\ell_2}{\dfrac{\partial F_0}{\partial L_2^*}} = \cdots \equiv \frac{d\ell_p}{\dfrac{\partial F_0}{\partial L_p^*}} = \frac{dS_1}{F_{1p}}. \tag{39}$$

Should one of the partials $\partial F_0/\partial L_i^*$ happen to be zero, the general solution would certainly be discontinuous since a "small divisor" is present. However this divisor is not exactly zero because the quantity $\partial F_0/\partial L_i^*$ is evaluated to first order only.

In the case of critical inclination it is necessary to take

$$S = S_0 + \epsilon^{1/2} S_{1/2} + \epsilon S_1 + \epsilon^{3/2} S_{3/2} + \cdots.$$

However, in doing so the separation of "long periodic" and "secular" perturbations is lost. The integration leads, in most cases, to elliptic integrals (Hori, 1960).

The question of small divisors usually arises whenever the problem presents cases of libration as particular solutions.

Another case to be mentioned is the resonance for an artificial satellite whose period is commensurable with the period of rotation of the Earth when tesseral harmonics are included. Again, expansion in powers of $\epsilon^{1/2}$ can be used to solve the problem (Morando, 1962).

Finally it is important to note that singularities in the Equations (39) reflect singular points in the hypersurface defined by the Hamiltonian of the system in a phase-space of $2(n-p)$ dimensions if p variables have already been eliminated.

7. SUMMARY

The general differential equations of the von Zeipel's method have been given to any order. It is hoped that this will avoid tedious Taylor expansions if one needs to go to order higher than the second.

At the same time, the brief discussion on the applicability and a few pathological cases of the method, may give some guidance toward the solution of new problems.

REFERENCES

1. Brouwer, D., Astron. J., **64**, 378–397, 1959.
2. Brouwer, D., Clemence, G., "Methods of Celestial Mechanics," Acad. Press, 1961.
3. Hori, G., Astron. J., **65**, 291, 1960.
4. Mello, S. F., Seminars of the Bureau des Longitudes, Paris, 1963.
5. Morando, B., Séance du 15 janvier 1962, Bureau des Longitudes, Paris.
6. Poincaré, H., "Les Méthodes Nouvelles de la Mécanique Céleste," Vol. I, Dover Publ., 1959.
7. Siegel, W., "Vorlesungen über Himmelsmechanik," Springer Verl., 1956.
8. Von Zeipel, H., Arkiv Mat., Astron., Physik, **11**, No. 1, 1916.